

Resource-constrained Project Scheduling with Time-of-Use Energy Tariffs and Machine States: A Logic-based Benders Decomposition Approach

Corentin Juvigny^a, Antonín Novák^a, Jan Mandík^a, Zdeněk Hanzálek^a

^a*Czech Institute of Informatics, Robotics and Cybernetics, Czech Technical University in Prague, Jugoslávských partyzánů 1580/3, 160 00, Prague 6, Czech Republic*

Abstract

In this paper, we investigate the Resource-Constrained Project Scheduling Problem (RCPSP) with time-of-use energy tariffs (TOU) and machine states, a variant of RCPSP for production scheduling where energy price is part of the criteria and one machine is highly energy-demanding and can be in one of the following three states: `proc`, `idle`, or `off`. The problem involves scheduling all tasks, respecting precedence constraints and resource limitations, while minimizing the combination of the overall makespan and the total energy cost (TEC), which varies according to the TOU pricing, which can take negative values. We propose two novel approaches to solve it: a *monolithic Constraint Programming* (CP) approach and a *Logic-Based Benders Decomposition* (LBBD) approach. The latter combines a master problem dealing with energy cost solved using Integer Linear Programming (ILP) with a subproblem handling the RCPSP resolved using CP. Both approaches surpass the *monolithic compact ILP* approach, but the LBBD significantly outperforms the CP when the ratio of energy-intensive tasks over the overall tasks is moderate, allowing for solving instances with up to 1600 tasks in sparse instances. Finally, we put forth a way of generalizing our LBBD approach to other problems sharing similar characteristics, and we applied it to a problem based on an RCPSP problem with blocking times & total weighted tardiness criterion and a flexible job shop.

Keywords: Resource-Constrained Project Scheduling Problems, Energy-price-aware Scheduling, Logic-based Benders Decomposition, Mixed-Integer Linear Programming, Constraint Programming

1. Introduction

The industrial sector is an important energy-demanding sector, accounting for around one-half of the world's total energy consumption, a share that has never stopped growing in recent years (Fang et al., 2011). The rising costs induced by energy production, combined with increasing concerns about the viability of intensified production as well as new public efforts fostering more durable production processes, have led an increasing number of studies to concentrate on energy-aware project scheduling (Du et al., 2021).

Email addresses: `corentin.juvigny@cvut.cz` (Corentin Juvigny), `antonin.novak@cvut.cz` (Antonín Novák), `zdenek.hanzalek@cvut.cz` (Zdeněk Hanzálek)

Time-of-use (TOU) pricing has emerged as a widely adopted strategy among energy suppliers of industrialized nations. This dynamic pricing mechanism serves two primary purposes: it facilitates the balancing of daily energy consumption patterns and mitigates peak load concentrations during specific hours (Hung and Michailidis, 2018; Chen and Zhang, 2019). It consists in adjusting electricity prices according to the fluctuation in demand, resulting in variable tariffs that can change quickly. This pricing structure provides consumers with significant opportunities to reduce their energy costs by shifting their major consumption activities to off-peak periods (Geng et al., 2020).

Moreover, for particularly energy-intensive operations, a more efficient management strategy may involve maintaining a machine in an intermediate state during the periods of inactivity, instead of completely shutting it down. Indeed, turning on a machine may consume a significant amount of energy and time. This is a case that can typically arise in industries operating furnaces or ovens. But the addition of these machine states leads to complex optimization problems (Benedikt et al., 2026).

However, in real industrial processes, not all operations are energy-intensive ones. They may be part of a more global project scheduling, with precedence constraints between the processes and limited capacities on resources involved, a category of scheduling problems called resource-constrained project scheduling problems (RCPSPs) (Herroelen et al., 1998).

To address these challenges, we study an RCPSP problem with time-of-use tariffs and machine states. Those states are modeled in a transition diagram, indicating the duration of the transitions between states and their associated energy consumptions. One of the resources of the RCPSP problem is defined as energy-intensive. We assume this energy-intensive resource has a unitary capacity, while the rest of the resources are less constrained on their associated capacity. We consider two objective functions. The first minimizes the total energy cost (TEC) induced by energy-intensive tasks regarding the TOU, and can be denoted as $PS, 1TOU|prec, states|TEC$. The second combines the previous TEC with a minimization of the makespan over all tasks. The extended Graham three-field notation (Graham et al., 1979) of this problem is $PS, 1TOU|prec, states|TEC, C_{max}$.

1.1. Paper contributions and outline

The main contributions of this article are the following.

- A new problem combining RCPSP with machine states and TOU is introduced. To model it, we detail two *monolithic* models, one based on *constraint programming* and one based on *integer linear programming*.
- A *Logic-based Benders decomposition* (LBBD) approach is put forth to solve the problem more efficiently. Experiments outline to what extent it outperforms the monolithic formulations, especially on the larger instances or when the subproblem can be reduced to a feasibility question.

- We propose a *generalization* of the LBBD approach to solve other optimization problems that exhibit close characteristics. In particular, we apply our LBBD approach to problems based on an RCPSP with blocking times & total weighted tardiness criterion ($PSm, 1TOU|intree, states|TEC, \sum_j w_j T_j$), as well as a flexible job shop ($FJm, 1TOU|prec, states|TEC, C_{max}$).

The following outline delineates the structure of the present study. Section 2 reviews the current state of the art of the literature. Section 3 details the problem and proposes a monolithic ILP formulation. Then, a constraint programming model is described in Section 4, while our novel LBBD approach is explained in Section 5. The proposed models are further assessed and compared in Section 6. Afterwards, Section 7 investigates the employment of our LBBD approach to other problems. Finally, Section 8 concludes the paper and exposes future avenues of research.

2. Literature Review

Resource-constrained project scheduling problems, first introduced by Wiest (1967), are widely studied strongly **NP-Hard** problems (Blazewicz et al., 1983). Both exact methods (Berthold et al., 2010; Chakrabortty et al., 2015) and heuristic approaches (Munlin, 2018; Pellerin et al., 2020) have been proposed to solve variants of this problem. Constraint programming has been unveiled as one of the most effective approaches for this kind of problem (Laborie et al., 2018). An extensive survey on this topic has recently been published by Artigues et al. (2025).

Energy-aware scheduling also gained popularity over the recent years. Most articles in the literature focus on minimizing energy costs under TOU energy pricing (Wan and Qi, 2010; Geng et al., 2020; Catanzaro et al., 2023). Although very specific shapes of the TOU pricing can make the problem polynomial (Fang et al., 2016), most real-world scenarios necessitate combining TOU with other scheduling problems, such as parallel machines (Ding et al., 2015; Gaggero et al., 2023), job shop (Kurniawan et al., 2021; Zhao et al., 2025), or flow shop (Ho et al. (2022)), making them much harder to solve. Some papers combine TEC with other metrics as well, such as makespan (Park and Ham, 2022; Gaggero et al., 2023) or tardiness (Rocholl et al., 2020; Kurniawan et al., 2021).

Fewer papers focus on RCPSP regarding energy consumption. Often, the energy consumption is linked to modes in the RCPSP where the most energy-intensive modes are faster (Zheng and Wang, 2015; Maghsoudlou et al., 2021; Pouramin et al., 2024). But none of them considers power-state machines on the energy-intensive resources. In this approach, machines can have, in addition to the processing state, other power-saving states (Aghelinejad et al., 2018). Shrouf et al. (2014) solved the $1, TOU|states|TEC$ problem using genetic algorithms, while Aghelinejad et al. (2019) showed that although the case with a fixed sequence of jobs can be solved in polynomial time, the unfixed version is strongly **NP-Hard**. Benedikt et al. (2020) introduced a shortest path based pre-processing technique called SPACES for $1TOU|states|C_{max}$ to

compute the optimal transitions of the machine states, leading to significantly faster integer linear programming/constraint programming models, compared to the initial compact ILP formulation proposed by Aghelinejad et al. (2018). Benedikt et al. (2026) proposed a novel branching scheme and diverse heuristics for $1\text{TOU}|\text{states}|C_{\max}$, outperforming the previous approach by two orders of magnitude. Zuccato et al. (2025) extended an Energy-Aware Double-Flexible Job Shop Scheduling Problem by incorporating machine modes, setup operations, and transport times based on an Austrian steel-cutting case study, proposing a Constraint Programming model to minimize tardiness, energy consumption, and makespan. Experimental results showed that higher resource flexibility improves solver performance, with CP successfully solving all instances in flexible scenarios while struggling with less flexible configurations, and demonstrating stronger performance in makespan optimization compared to tardiness minimization.

The Benders decomposition technique, introduced by Benders (1962), is a well-known and successful decomposition approach. It consists of decomposing large-scale mixed-integer programming problems into smaller, more manageable subproblems. It has been applied to many kinds of optimization problems, often with great success (Cordeau et al., 2000; Sherali et al., 2010; Alfandari et al., 2022; Juvigny et al., 2025). However, since the subproblems must be linear, this decomposition cannot be applied systematically to any kind of problem. Therefore, Hooker and Ottosson (2003) proposed a generalized version of the Benders decomposition, called Logic-based Benders Decomposition (LBBD). In the latter, the subproblems can be integer (Maschler and Raidl, 2017) or even non-linear ones, such as CP problems (Hooker et al., 2000; Thorsteinsson, 2001; Elçi and Hooker, 2022; Naderi and Roshanaei, 2022). Jain and Grossmann (2001) illustrated the efficiency of combining mixed-integer linear programming (MILP) with constraint programming for scheduling problems, achieving dramatic speedups over previous purely MILP approaches.

In summary, although some studies have investigated RCPSPs with TOU, none have considered the effect of adding machine states to the critical energetic resource. This problem can be seen as a generalization of the models previously proposed by Benedikt et al. (2020) and Benedikt et al. (2026).

In this paper, we will delve further into this LBBD approach by proposing new cuts tailored to our problem statement. We also show that any time-of-use problem sharing the same characteristics can benefit from our proposed method. Indeed, we demonstrate that our proposed method applies to a broader range of problems that involve state transitions, such as RCPSP with blocking periods and total weighted tardiness, or flexible job shops.

3. Problem statement

In this section, we describe the RCPSP with machine states and time-of-use (TOU) tariffs, along with its modeling by a compact monolithic ILP. Let us consider a *time horizon* $h \in \mathbb{N}$ divided into non-overlapping *unitary intervals* $\mathcal{I} = \{1, \dots, h\}$. Each interval is associated with an *energy cost* given by the vector

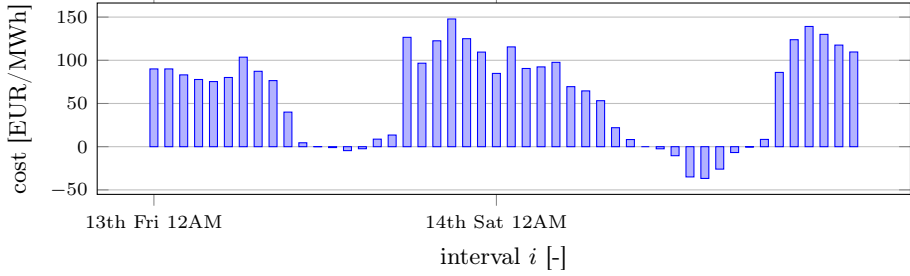


Figure 1: Example of a 48-hour part of the energy profile with real electricity costs in the day-ahead market in the Czech Republic from June 2025 provided by Czech OTE.

$c = (c_1, c_2, \dots, c_h) \in \mathbb{R}^h$. An example of a real energy cost profile is displayed in Figure 1.

Let $\mathcal{R} = \{R_0, R_1, \dots, R_m\}$ be a set of *resources*. We note ρ_k the *resource capacity* of a resource k . Let $\mathcal{T} = \{j_1, j_2, \dots, j_n\}$ be a set of *non-preemptive tasks* to be processed. To each task j is associated a *processing time* p_j and a *resource requirement* r_k^j , $k \in \mathcal{R}$. We want to calculate the *starting time* S_j of task j , from which we can induce its *completion time* $C_j = S_j + p_j$. For each resource, the sum of the resource requirements of tasks processed simultaneously shall not exceed the capacity of that resource, i.e., if we note $x_{ji} \in \{0, 1\}$ a binary decision variable equal to 1 when task j starts at time interval i and 0 otherwise:

$$\sum_{j \in \mathcal{T}} \sum_{i'=\max\{1, i-p_j+1\}}^i r_k^j x_{ji'} \leq \rho_k \quad \forall k \in \mathcal{R}, i \in \mathcal{I} \quad (3.1)$$

Indeed, in this time-indexed formulation, S_j of any task j is given by $S_j = \sum_{t \in \mathcal{I}} t x_{jt}$. Moreover, all the tasks have to be processed before the end of the time horizon:

$$\sum_{i \in \mathcal{I}} x_{ji} = 1 \quad \forall j \in \mathcal{T} \quad (3.2)$$

Additionally, let $G = (V, A)$ be the directed graph representing the *precedence constraints* between the tasks. Each node of G is a task of \mathcal{T} , and each arc $(v_j, v_{j'}) \in A$ means that task j precedes task j' , i.e., $S_j \geq C_{j'}$, and that:

$$\sum_{t \in \mathcal{I}} t x_{j't} - \sum_{t \in \mathcal{I}} t x_{jt} \geq p_j \quad \forall (j, j') \in A \quad (3.3)$$

We assume the resource R_0 to be the *energy-consumption significant*, also called *energy-intensive*, resource, with a capacity equal to 1. We note $\mathcal{J} \subset \mathcal{T}$, the subset of *energy-intensive tasks*, i.e., such that $\forall j \in \mathcal{J}, r_0^j > 0$. We consider this subset to be non-empty. We note $\bar{\mathcal{J}}$ its *complementary*, i.e., $\bar{\mathcal{J}} = \mathcal{T} \setminus \mathcal{J}$.

Until then, the formulation resembles a classical RCPSP problem. Now, let us introduce the variables and constraints that are specific to our problem. We consider that the resource R_0 has a *three-state set* $\Sigma = \{\text{proc, idle, off}\}$. During each time interval, the machine operates in one of these states. When an energy-intensive task is processed, the machine must be in *proc* state. We define a *transition time* function

$T : \Sigma \times \Sigma \rightarrow \mathbb{Z}_{>0} \cup \{\infty\}$ and a *transition energy* function $P : \Sigma \times \Sigma \rightarrow \mathbb{Z}_{\geq 0} \cup \{\infty\}$. We assume the transition time between two states cannot be null. A transition time of value ∞ between two states denotes that this transition is infeasible. Benedikt et al. (2020) have demonstrated that it is possible to precompute the optimal transition with respect to the energy cost between any two (proc state, interval) (as well as from the initial off state to any (proc state, interval), and from any (proc state, interval) to the final off state) thanks to a graph-based method they called *SPACES*. It consists of calculating the optimal transition between two (state, interval) as the shortest path between these states in the transition graph. Figure 4 pictures an example of the SPACES graph based on the parameters described in Figures 2 and 3. Let us note $\Omega = (\Omega_1, \Omega_2, \dots, \Omega_h)$ the vector that indicates for each time interval the current transition of the machine. For example, $\Omega_i = (\text{off}, \text{proc})$ means the machine is in transition from the off state at time i to the proc state at time $t + 1$, while $\Omega_{i'} = (\text{idle}, \text{idle})$ signifies the machine stays in the idle state between times i and i' . An optimal transition from an interval i to i' (assuming $i' > i$) in *SPACES* is therefore a vector containing the successive transitions with the lowest transition costs. If we denote z_{lm} the variable indicating that the machine is performing an optimal transition between the time intervals l and m , we can write the following constraints:

$$\sum_{j \in \mathcal{J}} \sum_{i'=\max\{1, i-p_j+1\}}^i x_{ji} + \sum_{l=1}^i \sum_{m=i+1}^{h+1} z_{lm} = 1 \quad \forall i \in \mathcal{I} \quad (3.4)$$

These constraints (3.4) signify that at each time interval, the machine is either processing a task (that is in proc, indicating by the fact that the processing of the task started in the $\max\{1, i - p_j + 1\}$ previous intervals) or undergoing an optimal transition. Furthermore, we assume this machine starts and ends in the off state, i.e.:

$$\sum_{i \in \text{StartTime} \cup \text{EndTime}} x_{ji} = 0 \quad \forall j \in \mathcal{J} \quad (3.5)$$

with $\text{StartTime} = \{1, \dots, 1 + T(\text{off}, \text{proc})\}$, $\text{EndTime} = \{h - T(\text{proc}, \text{off}) - p_j + 1, \dots, h\}$.

A *solution* is a pair (σ, Ω) where $\sigma = (\sigma_1, \sigma_2, \dots, \sigma_n) \in \mathbb{Z}_{\geq 0}^n$ is the vector denoting the start time of each task and $\Omega = (\Omega_1, \dots, \Omega_h) \in (\Sigma \times \Sigma)^h$ the vector of machine-state transitions. In summary, a solution is *feasible* if the following conditions are met:

- the resource capacities are not exceeded,
- the precedence constraints of each task are satisfied,
- the energy-demanding R_0 tasks are processed only when the R_0 machine is in proc state,
- the machine is off state during the first and last interval,
- transition between states s and s' takes $T(s, s')$ time intervals.

The total energy cost (TEC) of a solution (σ, Ω) can be computed as:

$$TEC = \sum_{i \in \mathcal{I}} c_i \cdot P(\Omega_i) \quad (3.6)$$

where for all $(s, s') = \Omega_i \in \Sigma^2$, $P(\Omega_i) = P(s, s')$.

We can compute the makespan C_{\max} of a solution as:

$$C_{\max} = \max_{j \in \mathcal{T}} C_j \quad (3.7)$$

We aim to minimize a convex combination of both objectives. For that, we introduce a real parameter $\alpha \in [0, 1]$ that represents the balance between the two. In order to have a better control over the balance between the two objective values, we normalize the individual objectives by their optimal solutions they would have if treated independently, i.e., the optimal makespan (lb_{RCPSP}) of the RCPSP problem for (3.7), and the optimal solution value for TEC (lb_{TEC}) when removing the non-energy-intensive tasks from the problem (however, their minimal impact on the energy-intensive tasks is preserved, that is, we update their precedence constraints and their computation times such that, if the removed tasks would be introduced in an optimal solution, but with an infinite resource capacity on all the resources but R_0 , they would fit between the energy-intensive tasks according to the precedence constraints). Note that these can be computed in practice efficiently — e.g., lb_{TEC} via an ILP of Benedikt et al. (2020) or by a branch and bound (Benedikt et al., 2026), whereas lb_{RCPSP} resembles a classical RCPSP problem that can be solved efficiently, e.g., by constraint programming (Heinz et al., 2025).

The objective function can therefore be written as:

$$\min \left\{ \alpha \cdot \frac{1}{lb_{TEC}} \cdot \sum_{i \in \mathcal{I}} c_i P(\Omega_i) + (1 - \alpha) \cdot \frac{1}{lb_{RCPSP}} \cdot C_{\max} \right\} \quad (3.8)$$

One can observe that when $\alpha = 0$, the objective function reduces to calculating the makespan, whereas when $\alpha = 1$, it involves finding the best TEC within the given time horizon. Thanks to the normalization, when $\alpha = 0.5$, both objectives weigh the same on the optimal solution. Thus, we can rewrite the objective function using our decision variables x and z as:

$$\min \frac{\alpha}{lb_{TEC}} \cdot \left(\sum_{j \in \mathcal{J}} \sum_{i=1}^h c_{ji}^{job} x_{ji} + \sum_{i=1}^h \sum_{j=1}^{h+1} c_{ij}^* z_{ij} \right) + \frac{(1 - \alpha)}{lb_{RCPSP}} \cdot \left(\sum_{t=1}^h t x_{n+1,t} + 1 \right) \quad (3.9)$$

where $c_{ji}^{job} = \sum_{k=i}^{i+p_j-1} c_k \cdot P(\text{proc}, \text{proc})$ is the cost of starting the job j at interval i , and c_{ij}^* is the cost of the optimal transition from interval i to interval j (see Benedikt et al. (2020) for more details). For computational reasons, we introduce a dummy task $n + 1$ which shall represent the makespan, associated with the constraints:

$$\sum_{t \in \mathcal{I}} t x_{(n+1)t} - \sum_{t \in \mathcal{I}} t x_{it} \geq 1 \quad \forall i \in \mathcal{T} \quad (3.10)$$

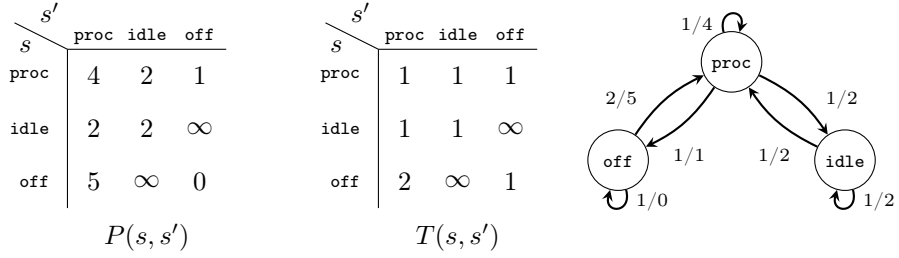
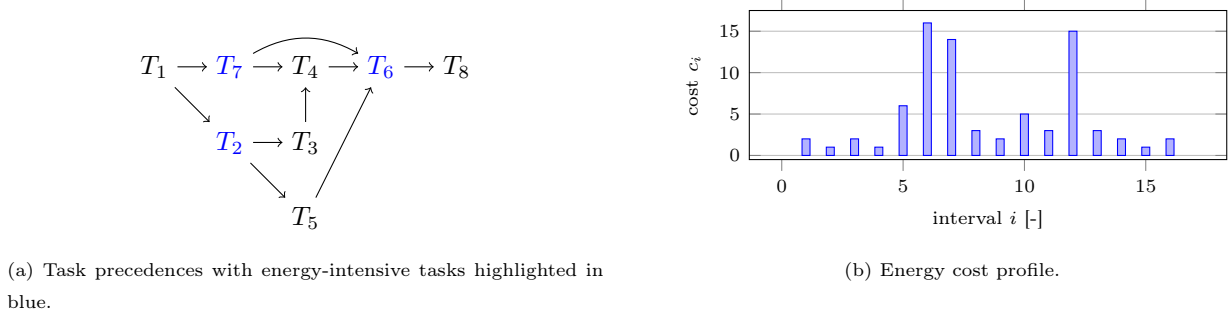


Figure 2: Parameters of the transition power function $P(s, s')$ and transition time function $T(s, s')$, and the corresponding transition graph, where every edge from s to s' is labeled by $T(s, s')/P(s, s')$.



parameters	T_1	T_2	T_3	T_4	T_5	T_6	T_7	T_8
p_i	2	1	2	1	3	2	2	2
R_0	0	1	0	0	0	1	1	0
R_1	5	0	2	3	2	0	0	3
R_2	2	0	1	1	2	0	0	2

Figure 3: Parameters for the example problem instance.

All the previous constraints associated with the objective (3.9) form a compact monolithic ILP model of the stated problem.

Example. Consider an instance with three resources $\{R_0, R_1, R_2\}$ and eight tasks $\mathcal{T} = \{T_1, \dots, T_8\}$ with a subset $\mathcal{J} = \{T_2, T_6, T_7\}$ of energy-intensive tasks. Precedence constraints are displayed in Figure 3a, processing times, and resource capacities of each task are detailed in Figure 3c. Figure 3b shows the TOU cost profile. We assume a transition diagram of resource R_0 as the one given in Figure 2. The corresponding SPACES graph is drawn in Figure 4. The optimal solution for the considered instance for $\alpha = 0.75$ is depicted in Figure 5.

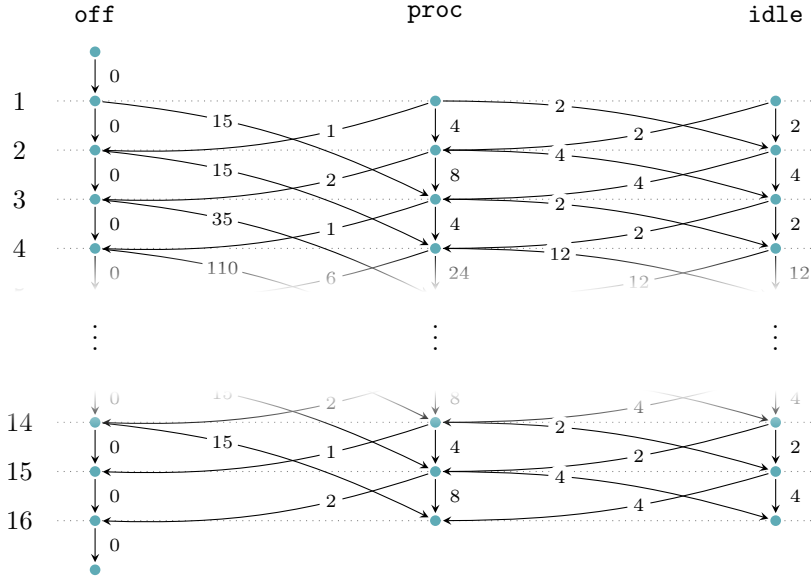


Figure 4: SPACES graph for the transition graph in Figure 2 and energy cost profile from Figure 3b.

4. Constraint programming model

In this section, we propose a model employing a constraint programming approach to solve the model defined in the previous section. In particular, we will take advantage of the fact that in the CP model, variables may or may not be present in the final solution, depending on the value of other given variables. Hence, we represent the optimal transitions between the energy-intensive tasks with variables of a fixed length that will be allowed to move around the schedule as necessary. This trick allows us to reduce the number of variables needed to represent the optimal transitions, as we can precisely compute the maximum number of optimal transitions of each length that can be used in the schedule. For the rest of the article, we will use the notations of the CP constraints defined in Heinz et al. (2022).

Variables. A new interval variable ξ_j of a fixed length p_j is created to represent each task $j \in \mathcal{T}$. This variable corresponds to the processing of a task j , starting at time $\text{STARTOF}(\xi_j)$ and ending at time $\text{ENDOF}(\xi_j)$. By definition, each interval variable must be scheduled. We introduce optional interval variables ζ_{lk} to represent the optimal transition in the spaces surrounding task processing on resource R_0 . Let $l_{\max} = h - \sum_{j \in \mathcal{T}} p_j$ be the upper bound on the optimal transition length. The function $K : l \mapsto \left\lfloor \frac{h - \sum_{j \in \mathcal{T}} p_j}{l} \right\rfloor$ then gives the upper bound on the number of optimal transitions of length l that can appear in the schedule. Therefore, the optional variables ζ_{lk} are created such that:

$$\text{LENGTHOF}(\zeta_{lk}) = l \quad \forall l \in \{1, \dots, l_{\max}\}, k \in \{1, \dots, K(l)\} \quad (4.1)$$

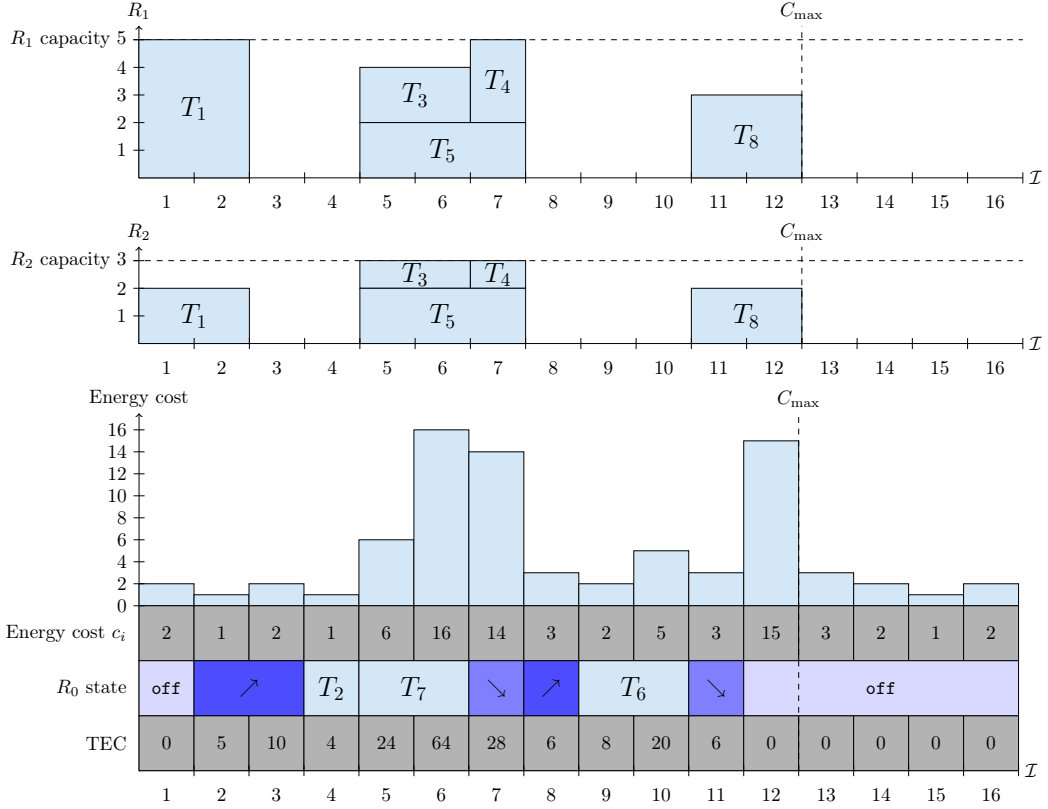


Figure 5: Example project schedule with the optimal transition for R_0 . Parameter $\alpha = 0.75$ (more towards TEC): $C_{max} = 12$, TEC = 172.

See an example in Figure 6 which displays interval variables present on resource R_0 in the solution corresponding to the Figure 5.

Objective. We use a vector c_j^{job} to express the total energy cost for the processing of task j based on the interval i it starts in. Additionally, since the variables representing the optimal switching are not fixed in their position, they are not directly associated with the total energy cost of the switching. Hence, we define the vector c_l^{space} , the i^{th} element of the vector corresponds to the total energy cost of the optimal switching of length l , if started in the interval i . The values of c_l^{space} are given as follows:

$$c_l^{space}[i] = c^*(i, i + l) \quad \forall i \in \{1, \dots, h - l + 1\}$$

The model minimizes the following objective:

$$\begin{aligned} \frac{\alpha}{lb_{TEC}} \cdot & \left(\sum_{l=1}^{l_{max}} \sum_{k=1}^{K(l)} \text{ELEMENT} (c_l^{space}, \text{STARTOF}(\zeta_{lk})) + \sum_{j \in \mathcal{J}} \text{ELEMENT} (c_j^{job}, \text{STARTOF}(\xi_j)) \right) \\ & + \frac{1 - \alpha}{lb_{RCPSP}} \cdot \max_{i \in \mathcal{T}} \{ \text{ENDOF}(\xi_i) \} \end{aligned} \quad (4.2)$$

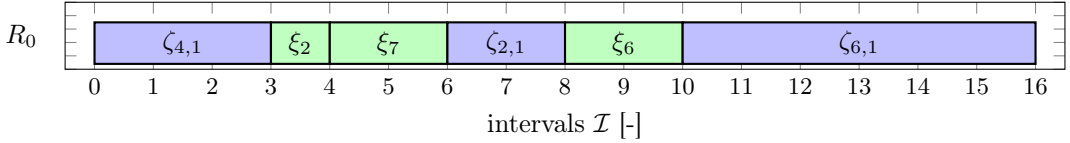


Figure 6: Interval variables present on resource R_0 in the solution from Figure 5.

with the first part representing the TEC part of the objective and the second part representing the C_{\max} part of the objective. Note that when computing the TEC, we consider only energy consumption-intensive tasks in the set \mathcal{J} , while for the C_{\max} objective, we consider all of the tasks.

Constraints. A solution is feasible if it respects the following constraints:

$$\text{STARTOF}(\zeta_{lk}) \geq 0 \quad \forall l \in \{1, \dots, l_{\max}\} \quad \forall k \in \{1, \dots, K(l)\} \quad (4.3)$$

$$\text{ENDOF}(\zeta_{lk}) \leq h \quad \forall l \in \{1, \dots, l_{\max}\} \quad \forall k \in \{1, \dots, K(l)\} \quad (4.4)$$

$$\text{PRESENCEOF}(\zeta_{lk}) \geq \text{PRESENCEOF}(\zeta_{lk+1}) \quad \forall l \in \{1, \dots, l_{\max}\}, k \in \{1, \dots, K(l) - 1\} \quad (4.5)$$

$$\text{ENDBEFORESTART}(\zeta_{lk}, \zeta_{lk+1}) \quad \forall l \in \{1, \dots, l_{\max}\}, k \in \{1, \dots, K(l) - 1\} \quad (4.6)$$

The constraints (4.3) and (4.4) ensure that all of the optimal transition variables, if present, are scheduled inside of the scheduling horizon. The constraints (4.5) and (4.6) give an ordering to the variables representing optimal transitions and ensure that the variables are used in an order given by their indexes for transitions of the same length. This removes redundant solutions that differ only in the order of variable use.

$$\text{STARTOF}(\xi_j) \geq 1 + T(\text{off}, \text{proc}) \quad \forall j \in \mathcal{J} \quad (4.7)$$

$$\text{ENDOF}(\xi_j) \leq h - T(\text{proc}, \text{off}) - 1 \quad \forall j \in \mathcal{J} \quad (4.8)$$

$$\text{ENDOF}(\xi_j) \leq h \quad \forall j \in \mathcal{T} \quad (4.9)$$

$$\text{NOOVERLAP}(\{\xi_j : \forall j \in \mathcal{J}\} \cup \{\zeta_{lk} : \forall l \in \{1, \dots, l_{\max}\}, k \in \{1, \dots, K(l)\}\}) \quad (4.10)$$

The constraints (4.7) and (4.8) ensure that all of the energy-intensive tasks are scheduled such that the energy-intensive machines have the time to warm up and shut down, respectively. Constraints (4.9) ensure that all of the tasks are scheduled inside the scheduling horizon. Compared to the constraints (4.7) and (4.8), we consider all of the tasks in this case. NOOVERLAP constraints (4.10) guarantee that the resource

R_0 is never processing a task and undergoing an optimal transition at the same time.

$$\sum_{l=1}^{l_{max}} \sum_{k=1}^{K(l)} \text{LENGTHOF}(\zeta_{lk}) = l_{max} \quad (4.11)$$

$$\sum_{j \in \mathcal{T}} \text{PULSE}(\xi_j, r_\kappa^j) \leq \rho_\kappa \quad \forall \kappa \in \mathcal{R} \quad (4.12)$$

$$\text{ENDBEFORESTART}(\xi_i, \xi_j) \quad \forall (i, j) \in A \quad (4.13)$$

The constraints (4.11) ensure that the length of all used optimal transitions in the solution is exactly equal to the value of l_{max} ; the optional variables that are not present in the solution do not count towards this sum. By the definition of l_{max} , these constraints, together with the constraints (4.10), also ensure that for the resource R_0 , the whole scheduling horizon is filled either by the processing of tasks or by optimal transitions in the spaces around. The constraints (4.12) guarantee that resource capacities are not exceeded at any time interval. Finally, with A being the set of arcs of the precedence graph, the constraints (4.13) rule out any solutions in which the precedence relations are violated.

5. Logic-Based Benders decomposition

This section introduces a novel LBBD approach for the studied problem, starting from its simplified version when $\alpha = 1$, to a general version for any $\alpha < 1$. The idea behind this approach is to separate the variables and constraints associated with the RCPSP problem from those related to the machine states problem. For that, at first, we will not consider the makespan in the objective. Therefore, the RCPSP part can be seen as a feasibility problem inside the TEC with TOU and machine states on a single machine. We then divide the problem into two dependent problems. The master one will be the machine state problem, solved by the ILP-SPACES model, while the subproblem will be an RCPSP feasibility problem modeled by a CP formulation. Of course, this would only work if $\alpha = 1$. Therefore, we will first present the special case $\alpha = 1$ in Section 5.1. Then, in Section 5.2, we will investigate how to generalize this approach to the case $\alpha < 1$. Note that the case $\alpha = 0$ is not interesting, and thus can be disregarded. Indeed, as long as the constraints (3.5) are satisfied, the machine state problem will not generate further infeasibility, since the machine can stay in `proc` state for the entire duration of the schedule. That means such a problem can be reduced to a classical RCPSP with a single time window on the energy-intensive tasks whose size should be nearly equal to the time horizon. The layout of our LBBD approach is detailed in Algorithm 1.

5.1. RCPSP seen as a feasibility problem: case $\alpha = 1$ (i.e., TEC only)

In this section, we consider that $\alpha = 1$, which means that only the total energy part of the objective function (3.8) matters. Therefore, the RCPSP can be seen as a feasibility problem.

Decision Variables

$x_{ji} = 1$ only if the task $j \in \mathcal{J}$ starts at interval $i \in \mathcal{I}$

$z_{ij} = 1$ only if the machine is performing an optimal SPACES transition between the intervals i and j

Table 1: Decision variables of the master problem ILP.

5.1.1. Master: modeled by ILP-SPACES

The master problem consists of optimizing the machine state problem alone, i.e., finding a scheduling of the energy-intensive tasks that minimizes the energy costs. Therefore, we keep in it all the constraints of the ILP related to the energy-intensive tasks. The decision variables, presented in Table 1, are similar to the ones of the ILP, except that only the energy-intensive tasks are represented by x_{ji} variables. All of the decision variables are binary. Hence, constraints (3.2), (3.3), (3.5), (3.4) and (3.1) (the latter limited to resource R_0) stay in the master. Constraints (3.10) are discarded since the makespan no longer has to be considered.

Let us introduce the relation ‘ \prec ’ for any $u, v \in \mathcal{T}$ such that $u \prec v$ denotes that u is a direct predecessor of v . We denote $\text{Pred}(j) \subset \mathcal{T}$ and $\text{Succ}(j) \subset \mathcal{T}$, the sets of the predecessors and the successors of a task j , respectively. The precedence constraints (3.3) cannot be used directly; indeed, since the binary variables x_{ji} represent only the energy-intensive tasks, if we consider $u, v \in \mathcal{J}$ and $j \in \overline{\mathcal{J}}$, then precedence constraints such as $u \prec j \prec v$ would not be taken into account. Furthermore, we know that in such a case $S_v \geq C_u + p_j$. Thus, for all $(u, v) \in \mathcal{J}^2$, if there exists a path $L_{uv} = \{j_1, \dots, j_l\}$ such that $u \prec j_1 \prec \dots \prec j_l \prec v$, then:

$$S_v \geq C_u + \sum_{j \in L_{uv}} p_j \quad (5.1)$$

Let \mathcal{L}_{uv} be the set of all precedence paths possible from task u to task v , i.e., if there exist L precedence paths possible between u and v , then $\mathcal{L}_{uv} = \{L_{uv}^l\}_{l \in \{1, \dots, \lambda\}}$. This set is finite since we have a finite number of tasks. We say that if $\mathcal{L}_{uv} \neq \emptyset$, then u is an ancestor of v , and v is a descendant of u . We name L_{uv}^* the longest path in \mathcal{L}_{uv} . Then, we can state that:

Proposition 1. *For any $(u, v) \in \mathcal{J}^2$, if $\mathcal{L}_{uv} \neq \emptyset$, then:*

$$S_v \geq C_u + \sum_{j \in L_{uv}^*} p_j \quad (5.2)$$

Proof. Let $(u, v) \in \mathcal{J}^2$ such that $\mathcal{L}_{uv} \neq \emptyset$. Therefore, there exist paths $L_{uv}^1, \dots, L_{uv}^\lambda$ in \mathcal{L}_{uv} . Without loss of generality, we can reorder them such that:

$$\sum_{j \in L_{uv}^1} p_j \leq \sum_{j \in L_{uv}^2} p_j \leq \dots \leq \sum_{j \in L_{uv}^\lambda} p_j$$

Therefore, according to (5.1), we have:

$$C_u + \sum_{j \in L_{ik}^1} p_j \leq \dots \leq C_u + \sum_{j \in L_{uv}^\lambda} p_j \leq S_v$$

Since by construction $L_{uv}^* = L_{uv}^\lambda$, Proposition 1 holds. \square

We introduce the function $MD : u \times v \in \mathcal{J}^2 \rightarrow \mathbb{Z}^+ \cup \{\infty\}$ such that $MD(u, v)$ is the minimal processing time between tasks u and v if v is a descendant of u , else ∞ , i.e.:

$$\forall u, v \in \mathcal{J}, \quad MD(u, v) = \begin{cases} p_u + \sum_{j \in L_{uv}^*} p_j & \text{if } \mathcal{L}_{uv} \neq \emptyset \\ \infty & \text{otherwise} \end{cases} \quad (5.3)$$

In fact, the domain of MD can be extended to the non-energy-intensive tasks $\overline{\mathcal{J}}$; this is useful because we should also take into account the cases where an energy-intensive task i has all of its predecessor tasks being non-energy-intensive ones, or similarly, when all of its successors are non-energy-intensive tasks. Computing this function is equivalent to calculating the longest paths between all nodes of the precedence graph associated with the RCPSP problem. Since there is no cyclic relation (i.e., $\nexists j \in \mathcal{T}, j \prec \dots \prec j$) in the RCPSP, the precedence graph is a directed acyclic graph. Hence, the longest paths can be found by computing the shortest paths in the precedence graph in which each arc leaving a node j has a weight equal to $-p_j$. Furthermore, as the precedence graph is usually sparse, we use Johnson's all-pairs shortest path algorithm (Johnson, 1977), which has a complexity of $O(|V||A|\log|V|)$ in a graph $G(V, A)$. We say that a task j is the predecessor (resp. successor) of a task i if $MD(i, j) < \infty$ (resp. $MD(j, i) < \infty$). In light of the above, the master ILP can be written as:

$$(Master) : \quad \min \sum_{j \in \mathcal{J}} \sum_{i=1}^h c_{ji}^{job} x_{ji} + \sum_{l=1}^h \sum_{m=1}^{h+1} c_{lm}^* z_{lm} \quad (5.4)$$

subject to

$$\sum_{i \in \mathcal{I}} x_{ji} = 1 \quad \forall j \in \mathcal{J} \quad (5.5)$$

$$\sum_{k \in \mathcal{I}} k x_{vk} - \sum_{k \in \mathcal{I}} k x_{uk} \geq MD(u, v) \quad \forall (u, v) \in \mathcal{J}^2, MD(u, v) < \infty \quad (5.6)$$

$$\sum_{j \in \mathcal{J}} \sum_{i'=\max\{1, i-p_j+1\}}^i x_{ji'} \leq 1 \quad \forall i \in \mathcal{I} \quad (5.7)$$

$$\sum_{i \in \text{StartTime} \cup \text{EndTime}} x_{ji} = 0 \quad \forall j \in \mathcal{J} \quad (5.8)$$

$$\sum_{j' \in \text{Pred}(j) \cup \overline{\mathcal{J}}} \sum_{i=0}^{MD(j', j)} x_{ji} + \sum_{j' \in \text{succ}(j) \cup \overline{\mathcal{J}}} \sum_{i=h-MD(j, j')+1}^h x_{ji} = 1 \quad \forall j \in \mathcal{J} \quad (5.9)$$

$$\sum_{j \in \mathcal{J}} \sum_{i'=\max\{1, i-p_j+1\}}^i x_{ji'} + \sum_{l=1}^i \sum_{m=i+1}^{h+1} z_{lm} = 1 \quad \forall i \in \mathcal{I} \quad (5.10)$$

Constraints (5.6) are a modified version of constraints (3.3) guaranteeing that each couple $(u, v) \in \mathcal{J}^2$ satisfies Proposition 1. Constraints (5.9) address scenarios where an energy-intensive task is preceded (resp. succeeded) by a sequence of non-energy-intensive tasks only. In this case, these constraints compel the energy-intensive task to allocate sufficient time before (resp. after) to allow this sequence to be scheduled. In fine, these two sets of constraints prune solutions that would have an associated subproblem that is trivially infeasible, without having the burden of verifying them. The rest of the constraints are similar to ILP constraints (however, restricted to set \mathcal{J} instead of \mathcal{T}).

However, an integer solution found by this master problem may not be a valid solution to our problem, as the resource constraints of non-energy-intensive tasks are not enforced. Therefore, each time a feasible solution is found, we verify the feasibility of its associated RCPSP problem in a subproblem; if the solution is not feasible, new constraints are added to cut off this solution.

5.1.2. Subproblem: modeled by CP

The subproblem consists of finding a feasible solution to the RCPSP problem associated with the solution provided by the master problem. Since the $\{x_{ji}\}_{j \in \mathcal{J}, i \in \mathcal{I}}$ are fixed integers in the subproblem, they impose the starting time of the energy-intensive tasks in the RCPSP. They shall be considered as parameters in the subproblem, denoted as $\{\hat{x}_{ji}\}_{j \in \mathcal{J}, i \in \mathcal{I}}$. Since it was reported by Heinz et al. (2025) that the constraint programming paradigm is highly efficient in finding solutions to RCPSPs, we will employ this approach to solve the subproblem. The proposed CP model is the following:

$$(Subproblem) : \sum_{j \in \mathcal{J}} \text{PULSE}(\xi_j, r_k^j) \leq \rho_k \quad \forall k \in \mathcal{R} \quad (5.11)$$

$$\text{ENDBEFORESTART}(\xi_i, \xi_j) \quad \forall (i, j) \in A \quad (5.12)$$

$$\text{ENDOF}(\xi_j) \leq h \quad \forall j \in \overline{\mathcal{J}} \quad (5.13)$$

$$\text{STARTOF}(\xi_j) = i \quad \forall j \in \mathcal{J}, i \in \mathcal{I}, \hat{x}_{ji} = 1 \quad (5.14)$$

$$\text{INTERVAL } \xi_j, \text{ LENGTHOF}(\xi_j) = p_j \quad \forall j \in \mathcal{T} \quad (5.15)$$

As in the monolithic CP described in Section 4, constraints (5.11) ensure that the capacities of each resource are not exceeded. Constraints (5.12) model the precedence constraints. Constraints (5.13) prevent the tasks from being scheduled after the end of the schedule horizon, while constraints (5.14) impose that the energy-intensive tasks start at the same time as in the master solution.

Additionally, instead of just finding a feasible solution, we can search for the RCPSP schedule that minimizes the makespan of the solution (indeed, the makespan of the RCPSP problem is the makespan of our problem in general), i.e.:

$$C_{\max}^{sub} : \min \max_{j \in \mathcal{T}} \text{ENDOF}(\xi_j) \quad (5.16)$$

In the particular case $\alpha = 1$, this objective function (5.16) does not need to be added to the CP, since our subproblem is therefore considered as a feasibility problem. However, at the end of the search, after an optimal solution has been found, it can be relevant to recompute its associated subproblem in view of the objective function, such that we could retrieve the optimal makespan of the master optimal solution (this is only for a practical perspective; it does not change anything on the optimal cost of the optimal solution).

When the subproblems cannot find a valid solution for a given energy-intensive task schedule given by the Master, we compute the minimal infeasibility set $\mathcal{I}nf \subseteq \mathcal{J}$ over the constraints (5.14). This set contains the variables appearing in the minimal conflict causing the infeasibility. Since the conflict is minimal, the removal of any one of these constraints will remove that particular cause for infeasibility. Note that there may exist other conflicts in the solution. This set can be computed automatically by the CP solver (Laborie et al., 2018) if it proves the infeasibility of the subproblem. However, in rare cases (which seem not to have occurred in our experiments), the solver cannot prove the infeasibility in a reasonable amount of time, thus preventing the calculation of $\mathcal{I}nf$. Once this set is found, the following cuts are added to the master.

Feasibility cuts. If $\mathcal{I}nf \neq \emptyset$, then we add the following feasibility cut:

$$\sum_{x_{ji} \in \mathcal{I}nf} x_{ji} \leq |\mathcal{I}nf| - 1 \quad (5.17)$$

This cut enforces that all but one of the energy-intensive tasks involved in the infeasibility set can keep their current starting time in a feasible solution. This shall rule out the current infeasible solution, while also pruning all solutions that share the same infeasible subset.

No good cuts. If $\mathcal{I}nf = \emptyset$, this means that the CP solver could not find an infeasibility set. In practice, this means that it can prove neither the feasibility nor the infeasibility of the master solution RCPSP subproblem, often due to a time limit. In that case, we just cut off this solution using the following no-good-cut constraint:

$$\sum_{j \in \mathcal{J}} \sum_{i \in \mathcal{I}} \hat{x}_{ji} x_{ji} \leq |\mathcal{J}| - 1 \quad (5.18)$$

This constraint is less efficient than constraint (5.17) because it only cuts this particular solution, meaning that any solution that would share a common cause of infeasibility with that solution shall also be computed and cut individually. However, this constraint is only in place as a backup constraint for cases where the feasibility of the constraint problem cannot be determined within a reasonable amount of time. In such a case, the optimality of the approach could no longer be guaranteed. Indeed, the solution could be, in the end, a feasible one, leading to an optimal solution being pruned. But, in practice, this case did not appear in our experiments, which had a 10-second time limit for the subproblem.

5.1.3. Warmstarts

An increase in instance size may undermine the efficacy of ILP approaches, thereby hindering their ability to find feasible solutions. Conversely, CP approaches are highly efficient in identifying feasible solutions quickly. However, these approaches often struggle to narrow the optimality gap due to their limited ability to generate strong lower bounds. Therefore, we propose two ways of generating a warmstart solution, both based on CP. The first uses the classical CP model (Artigues et al., 2013) with additional constraints (4.7) and (4.4). But we do not provide any objective function to the CP solver; the objective is just to find a valid solution. We call this warmstart approach *fsws*. The second solves the problem through the CP model delineated in Section 4, within a limited time frame of approximately one minute. We name this warmstart approach *cpws*. Subsequently, the optimal solution identified through these processes is utilized as a starting point for our ILP approaches, encompassing both the monolithic ILP and our LBBD.

5.2. Subproblem weighting on the master objective: case $\alpha < 1$ (i.e., TEC with C_{\max})

Now, let us focus on the case $\alpha < 1$. In this case, the C_{\max} objective function of the RCPSP also contributes to the objective function. Therefore, we need to introduce a way to represent the makespan inside the master problem. The issue is that, since most of the tasks of the RCPSP are not present in the master, we cannot induce the makespan directly from it.

Therefore, we introduce a new decision variable $q \in \mathbb{Z}_{\geq 0}$ to represent the value of the makespan. We rewrite the objective function as:

$$\min \frac{\alpha}{lb_{TEC}} \cdot \left(\sum_{j \in \mathcal{J}} \sum_{i=1}^h c_{ji}^{job} x_{ji} + \sum_{l=1}^h \sum_{m=1}^{h+1} c_{lm}^* z_{lm} \right) + \frac{1-\alpha}{lb_{RCPSP}} \cdot q \quad (5.19)$$

As described above, we require new constraints to ensure that the variable q accurately models the makespan. Since the latter is only known after computing the subproblem, we propose the following lazy optimality constraint:

$$obj_{sub}^* - M \left(|\mathcal{J}| - \sum_{j \in \mathcal{J}} \sum_{i \in \mathcal{I}} \hat{x}_{ji} x_{ji} \right) \leq q \quad (5.20)$$

where $obj_{sub}^* = C_{\max}^{sub}$ is the optimal makespan of the subproblem induced by $\{\hat{x}_{ji}\}$, and M is a big-M value. Given that the makespan of the subproblem is constrained to be no greater than the time horizon h , the tightest M is $h + 1$. That is the value we use in the present study.

These constraints only force the value of q for the integer solutions on which the subproblem has been computed. Obviously, they are only added when the subproblem is feasible; otherwise, lazy constraints (5.17) or (5.18) are added.

The inconvenience of this approach is that, since each constraint (5.20) (one per integer solutions found in the master and whose optimality has been proven) only imposes the makespan of a single integer solution,

it does not furnish any further information to the master problem, which is thus neither shepherded towards good solution candidates nor steered away from poor ones. However, we can estimate a lower bound on the value of the makespan considering the starting time of the energy-intensive tasks.

Proposition 2. *For all energy-intensive task $j \in \mathcal{J}$, the makespan q must satisfy the following constraints:*

$$\sum_{t \in \mathcal{I}} tx_{jt} + MD(j, s) + p_s \leq q \quad \forall s \in Succ(j) \quad (5.21)$$

Proof. The makespan of a solution of our problem cannot be less than the minimum amount of time required to process the consecutive tasks, i.e., as if the resource constraints of the RCPSP were ignored and only precedence constraints were present. Thus, we can deduce that, for each energy-intensive task j , a valid makespan must be at least equal to the largest minimum distances between j and its successors, i.e.:

$$\forall j \in \mathcal{J}, \forall s \in Succ(j), C_{\max} \geq S_j + MD(j, s) + p_s$$

Hence, we can infer from them the constraints (5.21). \square

These constraints (5.21) permit us to give a lower bound for the makespan in the master problem, considering the starting times of the energy-intensive tasks. They greatly help the convergence of our LBBD. Indeed, in fine, constraints (5.20) ultimately only come into play to correct an inaccurate estimate of the makespan, in cases where resource capacity constraints prevent tasks from being completed as quickly as they could be.

We conclude this section with some remarks. Our proposed LBBD approach guarantees the optimality of the final solution as long as all the subproblems have been either solved to optimality or proved infeasible. However, depending on the size or the complexity of the subproblem, it may be hard to prove either the feasibility or the optimality of *Subproblem* in a short time. In these cases, we proceed as follows: if *Subproblem* finds a feasible solution but cannot close the optimality gap, we insert in the *Master* an optimality constraint (5.20) where C_{\max}^{sub} is the best makespan found so far. On the contrary, when *Subproblem* can neither identify a feasible solution nor assert that no solution exists, we consider that the problem is infeasible, and we rule out the solution with a feasibility cut (5.18).

6. Experimental results

This section evaluates how the CP and LBBD models perform relative to the monolithic ILP model, which serves as our reference method. Section 6.1 describes the instance sets. Then, we present the results for case $\alpha = 1$ in Section 6.2. Section 6.3 exposes the results when $\alpha < 1$.

All experiments were run on 2 x AMD(R) EPYC(R) 9124 CPUs 3.5 GHz with 64 threads in total and 384 GB of RAM, running NixOS 25.05. Gurobi 12.0.2 and IBM CP Optimizer 22.1.1.0 are used to solve the

Algorithm 1 Logic-Based Benders Decomposition (LBB)

```
1: while Master is not optimal do
2:    $\hat{x} \leftarrow \text{Master}()$                                  $\triangleright$  Get integer solution.
3:    $\hat{\zeta} \leftarrow \text{Subproblem}(\hat{x})$                    $\triangleright$  Solve the subproblem.
4:   if  $\hat{\zeta}$  optimal or feasible then
5:     Add optimality cut (5.20) to Master                   $\triangleright$  Give feedback to the Master
6:   else
7:     Compute  $\mathcal{I}_{\text{Inf}}$                                  $\triangleright$  Retrieve tasks of  $\mathcal{J}$  that lead to infeasibility.
8:     if  $\mathcal{I}_{\text{Inf}} \neq \emptyset$  then
9:       Add feasibility cut (5.17) to Master                 $\triangleright$  Cut all solutions sharing same  $\mathcal{I}_{\text{Inf}}$  at once.
10:    else
11:      Add no-good cut (5.18) to Master                   $\triangleright$  Prune this specific solution from the Master.
12:    end if
13:  end if
14: end while
```

ILP and CP models, respectively. The code is written in C++20, compiled with Clang 19.1.7. We employ the Boost Graph Library (Siek et al., 2001) to implement graph components.

6.1. Dataset

We generated our instances based on the RCPSP instances of the standard PSPLIB dataset (Sprecher and Kolisch, 1996). To create an instance, we merged multiple small RCPSP instances of the PSPLIB together until we got an instance of the desired size. Then, we selected a given percentage of tasks in the newly created instance that we marked as “energy-intensive” (i.e., we set all of its other resource requirements to 0, then we added a requirement of 1 for R_0). We consider for each instance five resources R_0, \dots, R_4 . Finally, we generated a vector cost c of energy prices based on real TOU data collected from the Czech OTE¹. We can partition our test instances according to their ratio $\rho := |\mathcal{J}|/|\mathcal{T}|$ into three categories:

- Sparse instances: $\rho \approx 5\%$
- Standard instances: $\rho \approx 15 - 20\%$
- Dense instances: $\rho \approx 50\%$

For each of those categories, we generated instances of increasing sizes. Tables 2, 3b, and 3a provide details on the number of tasks and the time horizon for each set. For standard and dense instances, each set contains 20 instances, whereas for sparse instances, each set is made up of only one instance. The vector cost is unique

¹<https://www.ote-cr.cz/en>

for each instance. The datasets containing the sparse, standard, and dense instance sets are available at [dataset] Juvigny (2025e), [dataset] Juvigny (2025d), and [dataset] Juvigny (2025a), respectively.

Set	\mathcal{T}	\mathcal{J}				\mathcal{J} / \mathcal{T}	Horizon h			
		mean	min	max	std		mean	min	max	std
1	32	6.55	3	10	1.67	20.47	836.30	486	1117	150.19
2	64	11.60	8	15	1.64	18.12	963.95	740	1288	153.68
3	96	17.70	12	22	2.58	18.44	1297.70	928	1543	166.88
4	128	23.05	17	31	3.05	18.01	1672.35	1272	2055	225.03
5	160	29.70	23	35	3.66	18.56	1953.05	1601	2291	187.93
6	192	35.10	26	53	5.42	18.28	2306.45	1624	3228	397.50
7	224	40.65	35	47	3.54	18.15	2723.45	1999	3539	349.78
8	256	44.80	38	50	3.24	17.50	3039.45	2110	3757	411.91
9	288	51.40	42	60	5.48	17.85	3423.10	2670	3997	401.12
10	320	56.35	46	68	6.43	17.61	3816.95	2924	4517	509.27
11	352	59.25	52	69	3.70	16.83	4056.00	3445	4607	329.44
12	384	66.60	58	79	6.17	17.34	4406.70	3469	5710	531.31
13	416	71.95	61	85	5.95	17.30	4763.65	4180	6307	493.58
14	448	79.25	73	87	4.56	17.69	5202.85	4488	6066	389.12
15	480	85.75	74	97	7.37	17.86	5527.15	4513	6207	519.27

Table 2: Characteristics of standard instance sets. For each set, we present the number of tasks (| \mathcal{T} |), the number of energy-intensive tasks (| \mathcal{J} |), the ratio of energy-intensive tasks over the overall number of tasks (in %), and the time horizon. All instances of a set share the same number of tasks (std = standard deviation).

6.2. Case $\alpha = 1$, i.e., TEC only

We propose to compare the following methods: the monolithic ILP with a feasible warmstart (ILP-fs), ILP with a CP warmstart solution (ILP-cp), the proposed LBBD approach with a feasible warmstart solution (LBBD-fs) and with a CP warmstart solution (LBBD-cp), and the monolithic CP approach (CP). Both methods used to provide the warmstart solution are described in Section 5.1.3. The ILP-fs is our reference method, i.e., for any other method μ , we compute the delta to this reference method as:

$$\delta_\mu = \frac{obj_{ILP-fs} - obj_\mu}{obj_{ILP-fs}} \cdot 100 \quad (6.1)$$

Figure 8a presents the statistical distribution of the percentage of gain when $\alpha = 1$ for each instance set compared to the ILP-fs, of the methods listed above. It shows that in this case, the LBBD methods outperform the others, with solution deltas increasing as instance sizes grow. Moreover, it is also the method that optimally solves the largest number of instances before the time limit is reached, as shown by Figure 8b,

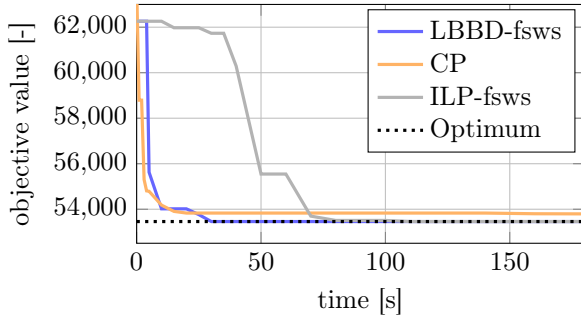
	$ \mathcal{T} $	$ \mathcal{J} $	$ \mathcal{J} / \mathcal{T} $	Horizon h
mean	128.00	65.00	51.16	4315.06
std	69.12	34.56	0.95	2313.90
min	32	17	50.45	1098.25
25%	80	41	50.57	2705.88
50%	128	65	50.78	4277.05
75%	176	89	51.30	5978.52
max	224	113	53.12	7461.30

(a) Summary statistics of dense instances.

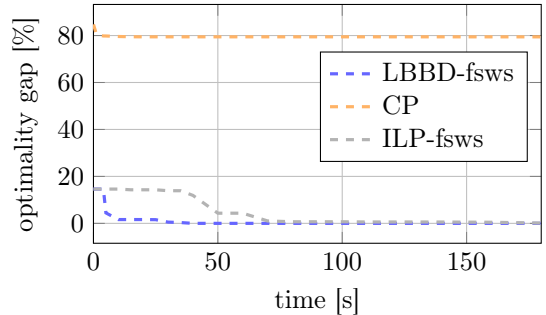
	$ \mathcal{T} $	$ \mathcal{J} $	$ \mathcal{J} / \mathcal{T} $	Horizon h
mean	816.00	26.58	3.47	5022.78
std	466.48	14.47	0.71	2587.64
min	32	2	3.19	851
25%	424	14.25	3.21	3066.50
50%	816	26.50	3.25	5235.50
75%	1208	38.75	3.36	6756.50
max	1600	51	7.03	10457

(b) Summary statistics of sparse instances.

Table 3: Summary statistics of large instances. $|\mathcal{J}|$ and $|\mathcal{T}|$ denote the number of energy-intensive tasks and the number of overall tasks, respectively. The ratio $|\mathcal{J}|/|\mathcal{T}|$ is reported in percentage.



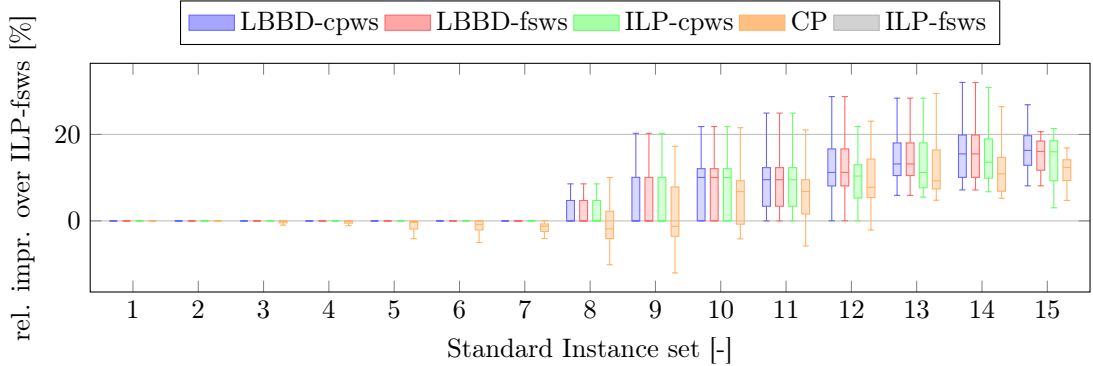
(a) Evolution of the upper bound (UB).



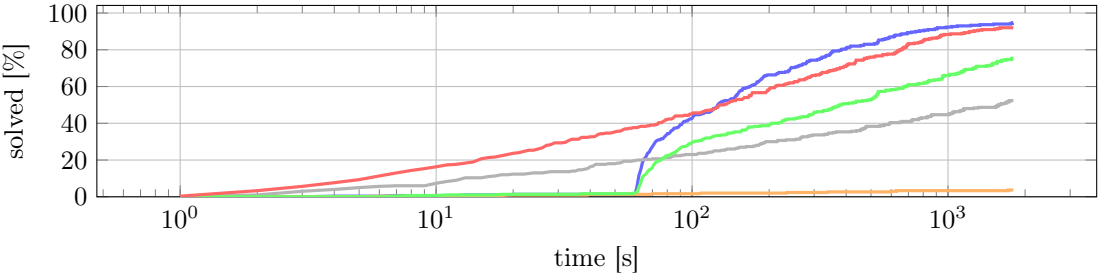
(b) Evolution of the gap of the best proven lower bound (LB).

Figure 7: Evolution of the UB and the optimality gap during the solution in standard instance 5_5 and $\alpha = 1$.

which displays the proportion of instances solved with proof of optimality over time. However, we can see from the figure that the methods using a CP warmstart have to wait 60 seconds for the CP computation before starting proving optimality. This means that the CP warmstart never proves the optimality of the solution, i.e., it never converges before reaching its time limit. In general, these figures indicate that the LBBD approach is consistently the best when the subproblem is only a feasibility problem, no matter the provided warmstart solution. They also learn us that the CP approach is, in that case, the one performing the worst, both in terms of computation times and of the best solution delta. In Figure 7, the evolution of the value of the upper bound (UB) and of the gap to the best proven lower bound (LB) of methods LBBD-fsfs, ILP-fsfs, and CP, for instance 5_5, is presented. This particular instance was selected due to its representativeness of the algorithms' behavior. We can see that the CP is the method having the steepest UB curve (see Figure 7a). The LBBD method follows closely behind, exhibiting a similarly sharp incline. This means that these approaches quickly converge to a good solution. On the contrary, the ILP takes more time to improve its UB. But, it ends up by finding and proving the optimal solution, as the LBBD



(a) Delta of the best solution each method found compared to the best solution found by the monolithic ILP with feasible warmstart.

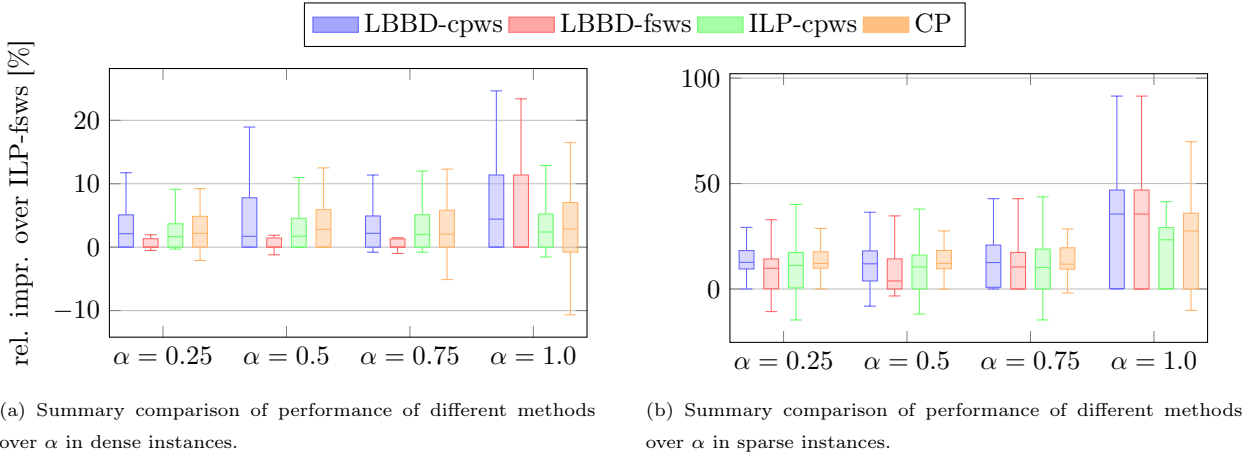


(b) Proportion of instances with proven optimality over time for the different methods.

Figure 8: Comparison when $\alpha = 1$ of different methods in the standard instance sets. A time limit of 1800 seconds is imposed.

does, whereas the CP gets stuck with a good but non-optimal solution, which seems unable to improve this solution. Indeed, its LB is very weak compared to the ILP approaches (Figure 7b). For information, in this instance, the LBBD-fs ws generates 18 feasibility cuts and 15 optimality cuts, with an average size of $\mathcal{I}nf$ of 1.333 variables. Moreover, for an overall computation time of 35 seconds, the solver passes around 0.6 seconds calculating the subproblems (considering that 33 subproblems were computed in total, this represents approximately 18 milliseconds per subproblem). Table 4 reports the average number of feasibility and optimality cuts added during the search by the LBBD. Its last row shows that when $\alpha = 1$, the average number of lazy cuts stays low; fewer than three solutions are eliminated by feasibility cuts, and less than ten others are examined. This is a reason for the high performance of the LBBDs in this case.

In sparse instances, the gap between the LBBD and the other approaches is even more important, as shown in Table B.6 and Figure 9b. We can notice that the one warmstarted by the CP model performs slightly better than the one warmstarted by a feasible solution. On the contrary, Figure 9a unveils that in dense instances, the LBBD approach with a feasible warmstart seems to dominate all the others, including the LBBD-cpws.



(a) Summary comparison of performance of different methods over α in dense instances.

(b) Summary comparison of performance of different methods over α in sparse instances.

Figure 9: Summary comparison of performance of different methods on instances of varying density of energy-intensive tasks.

6.3. Case $\alpha < 1$, i.e., TEC with C_{\max}

In this section, we study the more general case in which both the energy cost and the makespan influence the solution cost. We compare the same methods that previously for $\alpha \in \{0.25, 0.5, 0.75\}$. As mentioned earlier, we will not investigate the case $\alpha = 0$, because the problem would reduce to a standard RCPSP with as sole additional constraints (3.5). Figures 10, 11, and 12 present for each value of α the improvement δ_μ (6.1) of the solution objective compared to ILP-fsbs and the proportion of instances solved to proven optimality, for each instance set. They show that the two best approaches are our proposed LBBD approaches and the CP model. Moreover, the former is better to prove the optimality of the solutions, although only the smallest ones can be proven. Indeed, the problem ends up being far more difficult to solve than the case $\alpha = 1$ for all methods, with the monolithic ILPs being the most affected. The results displayed in Table 4 are interesting, because they reveal that the lower the α is, i.e., the more the makespan influences the overall cost, the higher the number of added lazy cuts. This is because, since the master is only guided by the TEC, the lower its impact, the more solutions it shall have to explore. Moreover, the size of an instance also impacts the number of lazy constraints explored, with smaller instances having higher lazy cuts in general. But this behavior could have been foretold, as having fewer variables in the master induces the latter can explore more integer solutions in the same amount of time. But, we would like to point out that this effect does not appear in the case of $\alpha = 1$, because in this case our approach is so effective that an optimal solution is found without the need to explore many feasible solutions. The LBBD approach performs best in sparse instances, as shown in Figure 9b and Table B.6. This behavior was expected, as the addition of non-energy-intensive tasks does not increase the size of the master problem, but is reflected only in the subproblem. On the contrary, the CP approach is more efficient in dense instances (see Figure 9a and Table B.7), where most of the benefit of our decomposition vanishes; furthermore, the LBBD tends to be the most memory-intensive method, limiting the model's capacity to solve large dense instances.

α	Feasibility cuts		Optimality cuts	
	LBBD-cpws		LBBD-fsbs	
	LBBB-cpws	LBBB-fsbs	LBBB-cpws	LBBB-fsbs
0.25	14.83	15.98	78.43	98.31
0.50	11.12	13.50	34.45	39.81
0.75	1.70	3.11	21.93	26.43
1.00	1.48	2.28	*6.43	*8.10

Table 4: Average number of feasibility and optimality cuts added by LBBD approaches per value of α over all the instance sets. (*when $\alpha = 1$, it only reports the average number of subproblems deemed feasible; no cut is added).

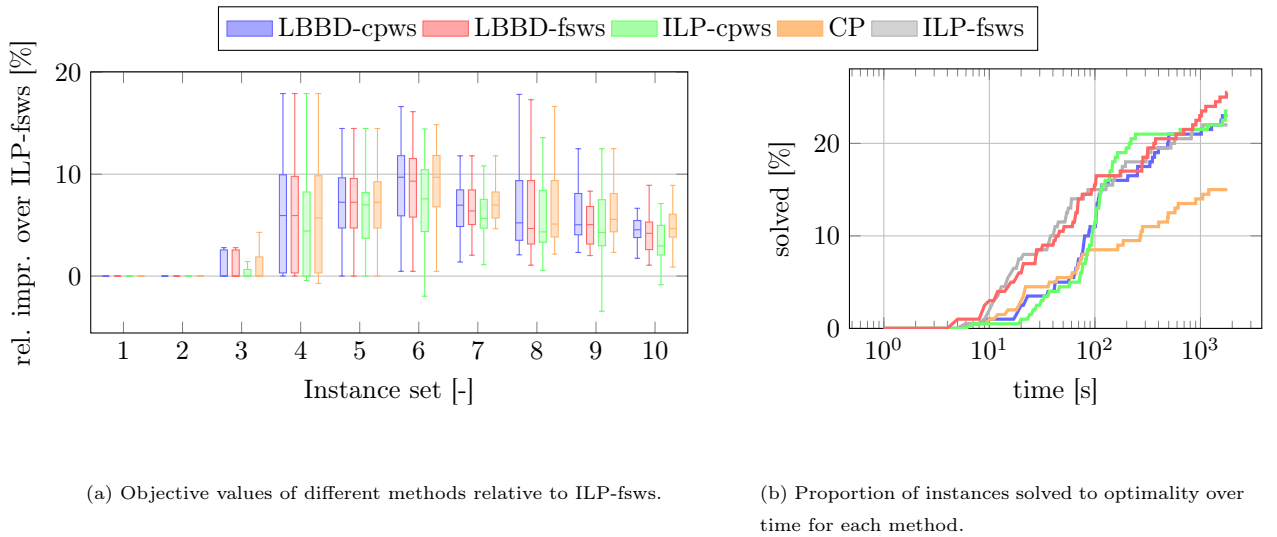


Figure 10: Comparison of different methods over the standard instance sets with $\alpha = 0.25$. A 1800-second time limit applies to all methods.

In summary, the outcomes reveal that the LBBD approach is well-suited to solve our problem, especially in cases where the number of energy-intensive tasks is low compared to the overall tasks. Indeed, by isolating the RCPSP part into a subproblem, additional non-energy-intensive tasks do not affect the resolution of the master. Moreover, we observe a benefit in most instances from providing a warmstart solution computed thanks to a one-minute run of our monolithic CP approach. Indeed, tests have shown that the latter converges quickly to a good solution, but then struggles to improve the latter.

7. Generalization to different resource environments

In this section, we investigate how our proposed decomposition scheme could be applied to other energy-aware problems with different machine environments. In particular, we present how to adapt our approach to two other scheduling problems: RCPSP with blocking times and the total weighted tardiness criterion,

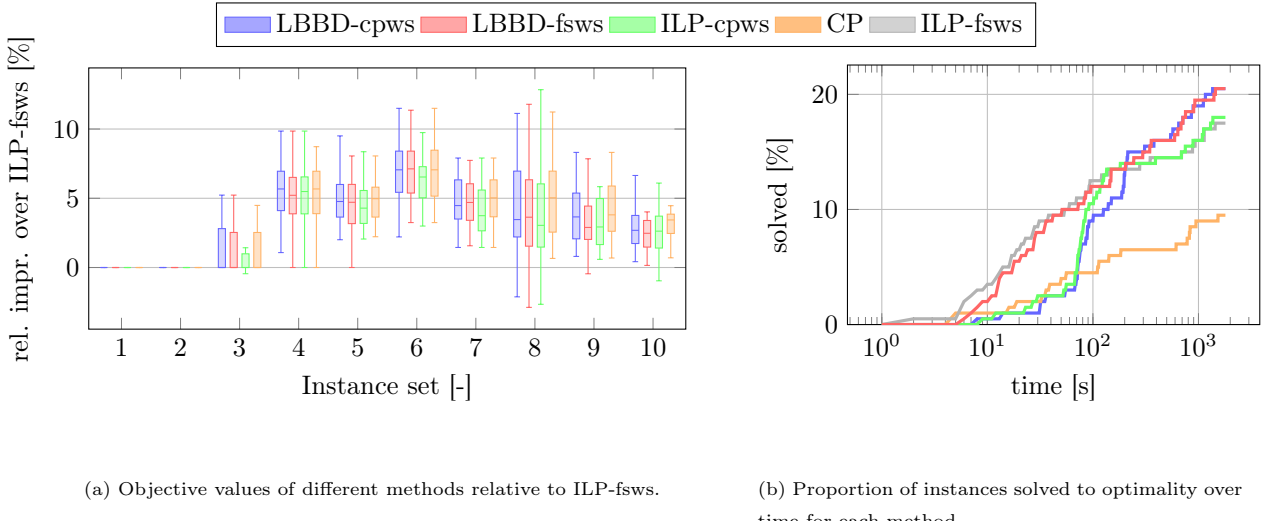


Figure 11: Comparison of different methods over the standard instance sets with $\alpha = 0.5$. A time limit of 1800 seconds is applied to all methods.

and a Flexible job shop. The two problems are combined with a time-of-use and machine states problem. We apply our decomposition approach to both. In the following, we detail only the subproblems, since the master problem is technically unchanged. Hence, the notations defined in Section 3 still hold.

7.1. Subproblem 1: RCPSP with blocking times & total weighted tardiness

In this section, we investigate another variant of the RCPSP, $PSm|intree|\sum_j w_j T_j$, detailed in Nedbálek and Novák (2025), which serves as the subproblem. In it, each task $j \in \mathcal{T}$ has a processing duration p_j and a due date d_j . We define the tardiness weight w_j as the penalty for each task j that is late in a given time period. The precedence constraints between tasks are represented by a graph $G = (V, A)$. Task preemption is not permitted. Tasks are assigned to resources $\mathcal{R} = \{R_0, \dots, R_m\}$ with time-variant renewable capacities, i.e., at any time $t \in \mathcal{I}$, the capacity of a resource k is $\rho_k^{(t)}$. We assume that $\rho_k^{(t)} \in \{0, r_k\}$ with $r_k > 0$, except for the energy-aware resource, which has a constant capacity of 1 at any time. At any time $t \in \mathcal{I}$, a task j would consume a quantity $r_{jk}^{(t)}$ of resource k if processed. The subproblem can be modeled by the following constraint programming formulation:

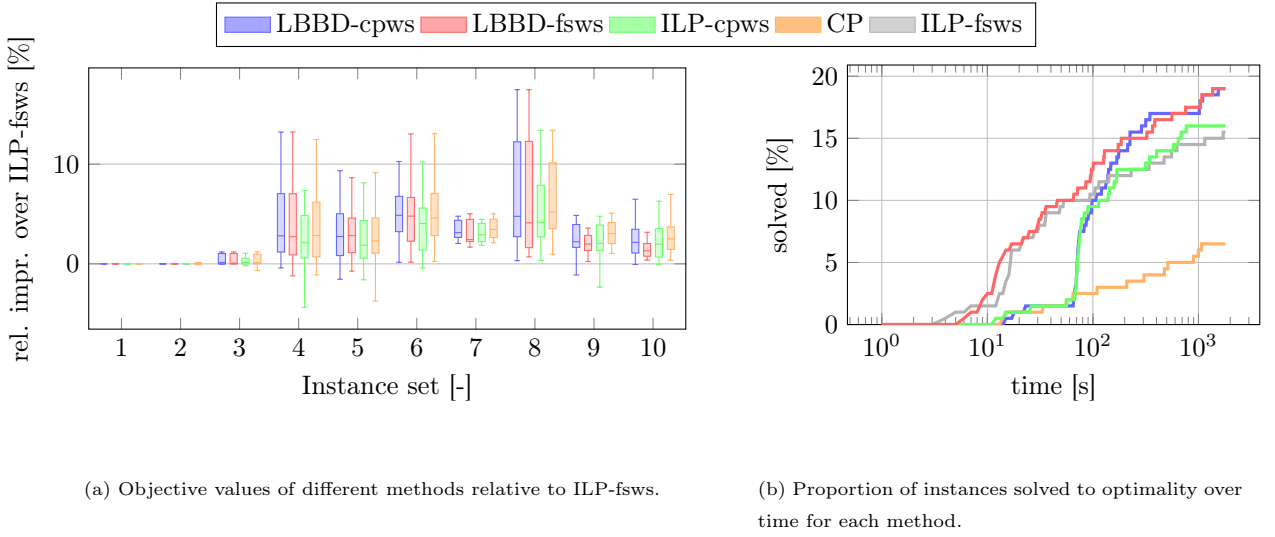


Figure 12: Comparison of different methods over the standard instance sets with $\alpha = 0.75$. A time limit of 1800 seconds is applied to all methods.

$$(Subproblem) : \min \sum_{j \in \mathcal{T}} w_j \max \{ \text{ENDOF}(\xi_j) - d_j, 0 \} \quad (7.1)$$

$$s.t. \quad \sum_{j \in \mathcal{T}} \text{PULSE} \left(\xi_j, r_{jk}^{(t)} \right) \leq \rho_k^{(t)} \quad \forall t \in \mathcal{I}, k \in \mathcal{R} \quad (7.2)$$

$$\text{ENDBEFORESTART}(\xi_i, \xi_j) \quad \forall (i, j) \in \mathcal{T}^2, i \prec j \quad (7.3)$$

$$\text{INTERVAL } \xi_j, \text{ LENGTHOF}(\xi_j) = p_j \quad \forall j \in \mathcal{T} \quad (7.4)$$

We compare our cold-started LBBB approach to a monolithic CP formulation derived from the CP proposed in Section 4 on a small set of instances derived from the dataset² proposed by Nedbálek and Novák (2025). For each instance, we randomly select 20% of the tasks to be energy-intensive. Table 5 presents, for different α values, the minimal, maximal, and average gaps (6.1) of the LBBB approach relative to the CP over the dataset, and the associated standard deviations. It reveals that our approach exhibits superior performance in terms of identifying optimal solutions when compared to the CP for all instances, with an average improvement of 7.68%, with a maximum reaching nearly 50%. It is also worth noting that the LBBB never performs worse than the CP. Furthermore, Figure 13 depicts how quickly our LBBB approach proves the optimality of solutions, with nearly 90% of instances solved to optimality in less than half an hour, whereas the CP could only prove the optimality of less than 5% of them in the same time.

²The dataset can be retrieved from [dataset] Juvigny (2025c)

α	Relative to CP [%]			
	mean	min	max	std
0.25	8.09	0.00	36.00	10.67
0.50	6.64	0.00	35.93	9.42
0.75	7.80	0.00	48.70	11.61
1.00	7.17	0.00	30.81	9.02

Table 5: RCPSP with blocking times & total weighted tardiness - Performance comparison for various values of α of the LBBB approach relative to the monolithic CP presented in Section 7.1. A time limit of 1800 seconds is imposed for both methods. std = standard deviation.

7.2. Subproblem 2: Flexible job shop

In this problem, we consider a classical flexible job shop problem (FJSP) $FJm||C_{\max}$ (Dauzère-Pérès et al., 2024). Let \mathcal{M} be a set of m machines. Each machine cannot handle more than one job at a time. We have a set of n jobs \mathfrak{J} . Each job $i \in \mathfrak{J}$ comprises a chain \mathcal{O}_i of operations $o_{i\lambda}$, thus, the set of all operations is $\mathcal{T} = \bigcup_{i \in \mathfrak{J}} \mathcal{O}_i$. Each operation i may be processed by a subset of machines $\mathcal{M}_i \subseteq \mathcal{M}$. We use the MILP detailed in Dauzère-Pérès et al. (2024). Let's the binary variables $\alpha_i^k = 1$ when operation i starts on machine k and $\beta_{ij} = 1$ when operation i is sequenced before j , and continuous variables C_{\max} and t_i , the subproblem MILP is:

$$(Subproblem) : \min C_{\max} \quad (7.5)$$

$$s.t. \quad \sum_{k \in \mathcal{M}_i} \alpha_i^k = 1 \quad \forall i \in \mathcal{T} \quad (7.6)$$

$$t_i \geq t_{pr(i)} + \sum_{k \in \mathcal{M}_{pr(i)}} p_{pr(i)}^m \alpha_{pr(i)}^k \quad \forall i \in \mathcal{T} \quad (7.7)$$

$$t_i \geq t_j + p_j^k - M (2 - \alpha_i^k - \alpha_j^k + \beta_{ij}) \quad \forall (i, j) \in \mathcal{T}^2, \text{ if } i \neq j, k \in \mathcal{M}_i \cap \mathcal{M}_j \quad (7.8)$$

$$t_j \geq t_i + p_i^k - M (3 - \alpha_i^k - \alpha_j^k - \beta_{ij}) \quad \forall (i, j) \in \mathcal{T}^2, \text{ if } i \neq j, k \in \mathcal{M}_i \cap \mathcal{M}_j \quad (7.9)$$

$$C_{\max} \geq t_i + \sum_{k \in \mathcal{M}_i} p_i^k \alpha_i^k \quad \forall i \in \mathcal{T} \quad (7.10)$$

$$t_j = t \quad \forall j \in \mathcal{J}, t \in \mathcal{I}, \hat{x}_{jt} = 1 \quad (7.11)$$

The overall objective function is normalized as in (3.8). We compare the LBBB with a monolithic MILP (detailed in Appendix A) based on the time-indexed formulation of the FJSP presented by Ku and Beck (2016). It is interesting to notice that the SPACES graph forces the monolithic ILP to follow a time-indexed formulation, while the subproblem of our LBBB can employ models that do not have to stick to this kind of

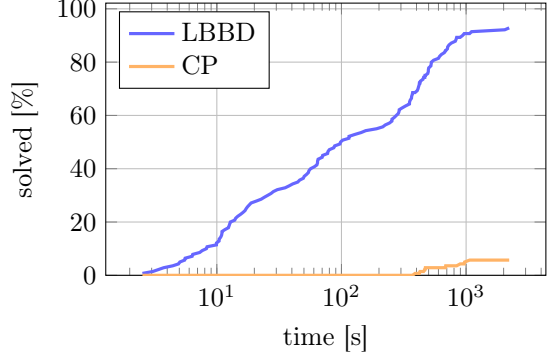


Figure 13: RCPSP with blocking times & total weighted tardiness - Proportion of instances solved to optimality by each method over time. The results for each value of $\alpha \in \{0.25, 0.5, 0.75, 1.0\}$ are concatenated.

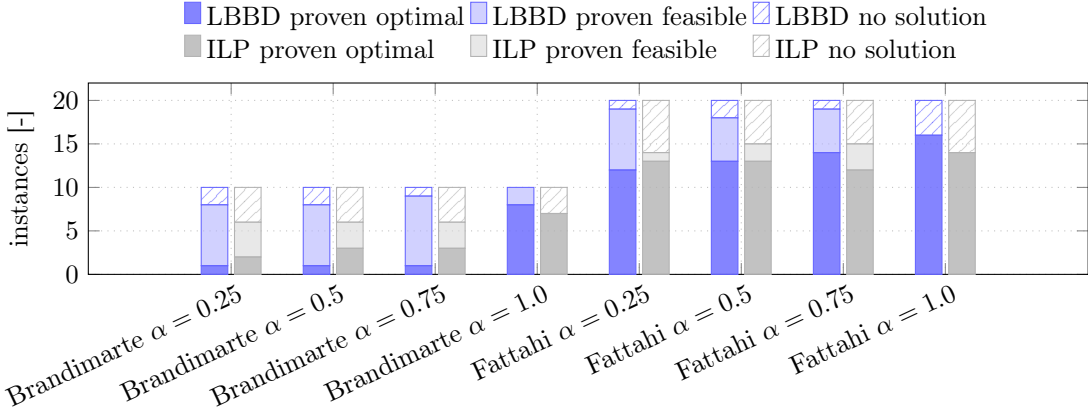


Figure 14: Flexible Job Shop - Number of solutions with proven optimality and feasible solution found grouped by benchmark set and α value.

formulation; in particular, the one we use in the subproblem does not. No warmstart solution is supplied to models. We employ the IIS (Irreducible Inconsistent Subsystem) (Gleeson and Ryan, 1990) provided by the solver to retrieve $\mathcal{I}nf$. The tests are performed on a dataset³ created from those of Brandimarte (1993) and Fattahi and Fallahi (2010), in which around 20% of the operations are set as energy-intensive. Figure 14 shows the number of instances in which LBBD and ILP have found an optimal solution for each dataset and each value of α . We observe that the ILP is better to prove optimality when α is low, while the LBBD is always better when $\alpha = 1$. Although the methods' performances remain close, ILP seems slightly better at proving the optimality of a solution in the other cases, especially in the Brandimarte set. But a general trend tends to emerge when the size of the instances grows, in which the LBBD digs out a feasible solution more often than the monolithic MILP. Indeed, as shown in Figure 14, over the 120 overall experiments run, with a time limit of 1800 seconds, the LBBD returned a feasible solution 107 times, while the monolithic ILP was only capable of finding one 83 times, i.e., around 20% less.

7.3. Additional remarks

In the problems mentioned in Section 7.1 and 7.2, our LBBD approach preserves the optimality of the final solution, as long as the subproblem is solved to optimality each time it is triggered. However, if this optimality criterion is not mandatory, approximation methods can be used to compute the subproblem. In particular, a wide variety of heuristics or metaheuristic approaches can be envisioned. They seem to be particularly suited for cases where the subproblem would be very complex, but only checks the feasibility of the master solution.

³The dataset can be retrieved from [dataset] Juvigny (2025b)

8. Conclusion

In this work, we investigated a classical resource-constrained project scheduling problem extended with time-of-use energy tariffs and machine states. We proposed three models for this problem: two monolithic models employing *ILP* and *CP* approaches, and an *LBBD*. In the latter, the problem is divided into two problems: a master problem, solved by an *ILP*, solves the energy part of the original problem, while the *RCPSp* components are put aside in a subproblem. This subproblem is solved efficiently via a *CP*. We assessed these models in a series of energy-intensive density instances. We showed that in sparse and standard instances, the *LBBD* approach outperforms the others, with increasing margins when the instance size grows. In high-density instances, the monolithic *CP* still seems to be the best, but not by far. Finally, we have exhibited that our *LBBD* approach can be applied to other kinds of problems, as long as they can be decomposed into an energy problem whose starting time of the energy-intensive tasks can be set in the subproblem. We tried two different subproblems: an *RCPSp* with blocking times and total weighted tardiness criterion, and a classical flexible job shop. For both, our *LBBD* approach surpasses a classical monolithic approach.

In further work, we can envision having multiple machines requiring energy-intensive resources. These machines may operate on the same energy source or require different energy-constrained resources, each with its own *TOU*. We can also consider a larger capacity of energy-intensive resources, rather than a unitary one. Furthermore, we can also consider more than three states, but with multiple idle/processing times, as some tasks require a precise state to be performed. We would also investigate the impact of temporary energy storage capacities, such as batteries, especially when combined with on-site energy production capacities (i.e., independent of time-of-use), such as solar panels. Finally, another avenue of research would be to explore the impact of introducing uncertainty in the energy price on our results and to investigate how to make schedules more resilient to such uncertainty.

CRediT authorship contribution statement

Corentin Juvigny: Conceptualization, Methodology, Investigation, Software, Writing - original draft
Antonín Novák: Conceptualization, Methodology, Investigation, Writing - original draft **Jan Mandík:** Conceptualization, Investigation **Zdeněk Hanzálek:** Conceptualization, Methodology, Investigation, Writing - original draft

Acknowledgments

This work was co-funded by the European Union under the project ROBOPROX (reg. no. CZ.02.01.01/00/22_008/0004590) and by the Grant Agency of the Czech Republic under the Project GACR 25-17904S.

References

Aghelinejad, M., Ouazene, Y., and Yalaoui, A. (2018). Production scheduling optimisation with machine state and time-dependent energy costs. *International Journal of Production Research*, 56(16):5558–5575.

Aghelinejad, M., Ouazene, Y., and Yalaoui, A. (2019). Complexity analysis of energy-efficient single machine scheduling problems. *Operations Research Perspectives*, 6:100105.

Alfandari, L., Ljubić, I., and Da Silva, M. D. M. (2022). A tailored benders decomposition approach for last-mile delivery with autonomous robots. *European Journal of Operational Research*, 299(2):510–525.

Artigues, C., Demassey, S., and Neron, E. (2013). *Resource-constrained project scheduling: models, algorithms, extensions and applications*. John Wiley & Sons.

Artigues, C., Hartmann, S., and Vanhoucke, M. (2025). Fifty years of research on resource-constrained project scheduling explored from different perspectives. *European Journal of Operational Research*.

Benders, J. (1962). Partitioning procedures for solving mixed-variables programming problems. *Numer. Math.*, 4(1):238–252.

Benedikt, O., Módos, I., and Hanzálek, Z. (2020). Power of pre-processing: production scheduling with variable energy pricing and power-saving states. *Constraints*, 25(3):300–318.

Benedikt, O., Módos, I., Novak, A., and Hanzálek, Z. (2026). Green scheduling with time-of-use tariffs and machine states: Optimizing energy cost via branch-and-bound and bin packing strategies. *European Journal of Operational Research*, 328(1):64–77.

Berthold, T., Heinz, S., Lübbecke, M. E., Möhring, R. H., and Schulz, J. (2010). A constraint integer programming approach for resource-constrained project scheduling. In *International Conference on Integration of Artificial Intelligence (AI) and Operations Research (OR) Techniques in Constraint Programming*, pages 313–317. Springer.

Blazewicz, J., Lenstra, J. K., and Kan, A. R. (1983). Scheduling subject to resource constraints: classification and complexity. *Discrete applied mathematics*, 5(1):11–24.

Brandimarte, P. (1993). Routing and scheduling in a flexible job shop by tabu search. *Annals of Operations research*, 41(3):157–183.

Catanzaro, D., Pesenti, R., and Ronco, R. (2023). Job scheduling under time-of-use energy tariffs for sustainable manufacturing: a survey. *European Journal of Operational Research*, 308(3):1091–1109.

Chakrabortty, R. K., Sarker, R., and Essam, D. (2015). Resource constrained project scheduling: A branch and cut approach. In *Proceedings of the 45th international conference on computers and industrial engineering Metz*, volume 132.

Chen, B. and Zhang, X. (2019). Scheduling with time-of-use costs. *European Journal of Operational Research*, 274(3):900–908.

Cordeau, J.-F., Soumis, F., and Desrosiers, J. (2000). A benders decomposition approach for the locomotive and car assignment problem. *Transportation science*, 34(2):133–149.

[dataset] Juvigny, C. (2025a). Dense instances for RCPSP with time-of-use tariffs and machine states.

[dataset] Juvigny, C. (2025b). Instances for FJSP with time-of-use tariffs and machine states.

[dataset] Juvigny, C. (2025c). Instances for RCPSP with blocking times & machine states & TOU & total weighted tardiness criteria.

[dataset] Juvigny, C. (2025d). Instances of standard density for RCPSP with time-of-use tariffs and machine states.

[dataset] Juvigny, C. (2025e). Sparse instances for RCPSP with time-of-use tariffs and machine states.

Dauzère-Pérès, S., Ding, J., Shen, L., and Tamssouet, K. (2024). The flexible job shop scheduling problem: A review. *European Journal of Operational Research*, 314(2):409–432.

Ding, J.-Y., Song, S., Zhang, R., Chiong, R., and Wu, C. (2015). Parallel machine scheduling under time-of-use electricity prices: New models and optimization approaches. *IEEE Transactions on Automation Science and Engineering*, 13(2):1138–1154.

Du, B., Tan, T., Guo, J., Li, Y., and Guo, S. (2021). Energy-cost-aware resource-constrained project scheduling for complex product system with activity splitting and recombining. *Expert Systems with Applications*, 173:114754.

Elçi, Ö. and Hooker, J. (2022). Stochastic planning and scheduling with logic-based benders decomposition. *INFORMS Journal on Computing*, 34(5):2428–2442.

Fang, K., Uhan, N., Zhao, F., and Sutherland, J. W. (2011). A new approach to scheduling in manufacturing for power consumption and carbon footprint reduction. *Journal of Manufacturing Systems*, 30(4):234–240.

Fang, K., Uhan, N. A., Zhao, F., and Sutherland, J. W. (2016). Scheduling on a single machine under time-of-use electricity tariffs. *Annals of Operations Research*, 238(1):199–227.

Fattah, P. and Fallahi, A. (2010). Dynamic scheduling in flexible job shop systems by considering simultaneously efficiency and stability. *CIRP Journal of Manufacturing Science and Technology*, 2(2):114–123.

Gaggero, M., Paolucci, M., and Ronco, R. (2023). Exact and heuristic solution approaches for energy-efficient identical parallel machine scheduling with time-of-use costs. *European Journal of Operational Research*, 311(3):845–866.

Geng, K., Ye, C., Dai, Z. H., and Liu, L. (2020). Bi-objective re-entrant hybrid flow shop scheduling considering energy consumption cost under time-of-use electricity tariffs. *Complexity*, 2020(1):8565921.

Gleeson, J. and Ryan, J. (1990). Identifying minimally infeasible subsystems of inequalities. *ORSA Journal on Computing*, 2(1):61–63.

Graham, R., Lawler, E., Lenstra, J., and Kan, A. (1979). Optimization and approximation in deterministic sequencing and scheduling: a survey. In Hammer, P., Johnson, E., and Korte, B., editors, *Discrete Optimization II*, volume 5 of *Annals of Discrete Mathematics*, pages 287–326. Elsevier.

Heinz, V., Novák, A., Vlk, M., and Hanzálek, Z. (2022). Constraint programming and constructive heuristics for parallel machine scheduling with sequence-dependent setups and common servers. *Computers & Industrial Engineering*, 172:108586.

Heinz, V., Vilím, P., and Hanzálek, Z. (2025). Reinforcement learning for search tree size minimization in constraint programming: New results on scheduling benchmarks. *Computers & Industrial Engineering*, 209:111413.

Herroelen, W., De Reyck, B., and Demeulemeester, E. (1998). Resource-constrained project scheduling: A survey of recent developments. *Computers & Operations Research*, 25(4):279–302.

Ho, M. H., Hnaien, F., and Dugardin, F. (2022). Exact method to optimize the total electricity cost in two-machine permutation flow shop scheduling problem under time-of-use tariff. *Computers & Operations Research*, 144:105788.

Hooker, J., Ottosson, G., Thorsteinsson, E. S., and Kim, H.-J. (2000). A scheme for unifying optimization and constraint satisfaction methods. *The Knowledge Engineering Review*, 15(1):11–30.

Hooker, J. N. and Ottosson, G. (2003). Logic-based benders decomposition. *Mathematical Programming*, 96(1):33–60.

Hung, Y.-C. and Michailidis, G. (2018). Modeling and optimization of time-of-use electricity pricing systems. *IEEE transactions on smart grid*, 10(4):4116–4127.

Jain, V. and Grossmann, I. E. (2001). Algorithms for hybrid milp/cp models for a class of optimization problems. *INFORMS Journal on computing*, 13(4):258–276.

Johnson, D. B. (1977). Efficient algorithms for shortest paths in sparse networks. *Journal of the ACM (JACM)*, 24(1):1–13.

Juvigny, C., Alfandari, L., and Delle Donne, D. (2025). Genetic and benders approaches for operational freight-on-transit problems with robot delivery. *Available at SSRN 5400671*.

Ku, W.-Y. and Beck, J. C. (2016). Mixed integer programming models for job shop scheduling: A computational analysis. *Computers & Operations Research*, 73:165–173.

Kurniawan, B., Song, W., Weng, W., and Fujimura, S. (2021). Distributed-elite local search based on a genetic algorithm for bi-objective job-shop scheduling under time-of-use tariffs. *Evolutionary Intelligence*, 14(4):1581–1595.

Laborie, P., Rogerie, J., Shaw, P., and Vilím, P. (2018). Ibm ilog cp optimizer for scheduling: 20+ years of scheduling with constraints at ibm/ilog. *Constraints*, 23(2):210–250.

Maghsoudlou, H., Afshar-Nadjafi, B., and Niaki, S. T. A. (2021). A framework for preemptive multi-skilled project scheduling problem with time-of-use energy tariffs. *Energy Systems*, 12(2):431–458.

Maschler, J. and Raidl, G. R. (2017). A logic-based benders decomposition approach for the 3-staged strip packing problem. In *Operations Research Proceedings 2015: Selected Papers of the International Conference of the German, Austrian and Swiss Operations Research Societies (GOR, ÖGOR, SVOR/ASRO), University of Vienna, Austria, September 1-4, 2015*, pages 393–399. Springer.

Munlin, M. (2018). Solving resource-constrained project scheduling problem using metaheuristic algorithm. In *2018 5th International Conference on Electrical and Electronic Engineering (ICEEE)*, pages 344–349. IEEE.

Naderi, B. and Roshanaei, V. (2022). Critical-path-search logic-based benders decomposition approaches for flexible job shop scheduling. *INFORMS Journal on Optimization*, 4(1):1–28.

Nedbálek, L. and Novák, A. (2025). Bottleneck identification in resource-constrained project scheduling via constraint relaxation. In *Proceedings of the 14th International Conference on Operations Research and Enterprise Systems - ICORES*, pages 340–347. INSTICC, SciTePress.

Park, M.-J. and Ham, A. (2022). Energy-aware flexible job shop scheduling under time-of-use pricing. *International Journal of Production Economics*, 248:108507.

Pellerin, R., Perrier, N., and Berthaut, F. (2020). A survey of hybrid metaheuristics for the resource-constrained project scheduling problem. *European journal of operational research*, 280(2):395–416.

Pouramin, M., Mirzazadeh, A., Davari-Ardakani, H., Mosadegh, H., and Alajegerdi, E. (2024). Multi-mode resource-constrained project scheduling problem along with material ordering under time-of-use electricity tariffs and carbon taxes. *Annals of Operations Research*, pages 1–45.

Rocholl, J., Mönch, L., and Fowler, J. (2020). Bi-criteria parallel batch machine scheduling to minimize total weighted tardiness and electricity cost. *Journal of Business Economics*, 90(9):1345–1381.

Sherali, H. D., Bae, K.-H., and Haouari, M. (2010). Integrated airline schedule design and fleet assignment: Polyhedral analysis and benders' decomposition approach. *INFORMS Journal on Computing*, 22(4):500–513.

Shrouf, F., Ordieres-Meré, J., García-Sánchez, A., and Ortega-Mier, M. (2014). Optimizing the production scheduling of a single machine to minimize total energy consumption costs. *Journal of Cleaner Production*, 67:197–207.

Siek, J. G., Lee, L.-Q., and Lumsdaine, A. (2001). *The Boost Graph Library: User Guide and Reference Manual*. Pearson Education.

Sprecher, A. and Kolisch, R. (1996). Psplib-a project scheduling problem library. *European Journal of Operational Research*, 96(1):205–216.

Thorsteinsson, E. S. (2001). Branch-and-check: A hybrid framework integrating mixed integer programming and constraint logic programming. In *International conference on principles and practice of constraint programming*, pages 16–30. Springer.

Wan, G. and Qi, X. (2010). Scheduling with variable time slot costs. *Naval Research Logistics (NRL)*, 57(2):159–171.

Wiest, J. D. (1967). A heuristic model for scheduling large projects with limited resources. *Management Science*, 13(6):B–359.

Zhao, S., Zhou, H., Chu, F., Wang, D., and Gao, K. (2025). A twin-reinforced evolutionary algorithm for flexible job shop scheduling problem under time-of-use tariffs. *Computers & Industrial Engineering*, page 111754.

Zheng, H.-y. and Wang, L. (2015). Reduction of carbon emissions and project makespan by a pareto-based estimation of distribution algorithm. *International Journal of Production Economics*, 164:421–432.

Zuccato, F., Rodler, P., Friedrich, G., Schekotihin, K., and Comploi-Taupe, R. (2025). Energy-aware double-flexible job shop scheduling with machine modes and setup times: A real-world industrial case study using constraint programming.

Appendix A. Monolithic MILP formulation for Flexible Job Shop with Machine states and TOU

The following monolithic MILP models the Flexible Job Shop with Machine states and TOU problem. The binary decision variable $x_{jt}^k = 1$ only if an operation $j \in \mathcal{T}$ starts on machine $k \in \mathcal{M}_j$ at time $t \in \mathcal{I}$.

$$\min C_{\max} \quad (A.1)$$

$$s.t. \quad \sum_{t \in \mathcal{I}} \sum_{k \in \mathcal{M}_i} x_{jt}^k = 1 \quad \forall j \in \mathcal{T} \quad (A.2)$$

$$\sum_{t \in \mathcal{I}} \sum_{k_j \in \mathcal{M}_j} x_{jt}^{k_j} - \sum_{t \in \mathcal{I}} \sum_{k_i \in \mathcal{M}_i} (t + p_i^{k_i}) x_{it}^{k_i} \geq 0 \quad \forall (i, j) \in \mathcal{T} \times \mathcal{T}, i \prec j \quad (A.3)$$

$$\sum_{j \in \mathcal{T} | k \in \mathcal{M}_j} \sum_{l=\max\{1, t-p_j^k+1\}}^t x_{jl}^k \leq 1 \quad \forall k \in \mathcal{M}, t \in \mathcal{I} \quad (A.4)$$

$$\sum_{j \in \mathcal{J}} x_{ji}^{k_0} = 0 \quad \forall i \in \text{StartTime} \cup \text{EndTime} \quad (A.5)$$

$$\sum_{j \in \mathcal{J}} \sum_{t'=\max\{1, t-p_j^{k_0}+1\}}^{t+1} x_{jt'}^{k_0} + \sum_{l=1}^{t+1} \sum_{m=t+1}^{h+1} z_{lm} = 1 \quad \forall t \in \mathcal{I} \quad (A.6)$$

$$\sum_{t \in \mathcal{I}} \sum_{k \in \mathcal{M}_j} (t + p_j^k) x_{jt}^k \leq C_{\max} \quad \forall j \in \mathcal{T} \quad (A.7)$$

Constraints (A.2) ensure all operations are scheduled. Constraints (A.3) monitor the precedence constraints, while constraints (A.4) prevent more than one operation from being performed simultaneously on the same machine. Constraints (A.5) and (A.6) represent the machine state part of the problem. Finally, constraints (A.7) track the makespan (A.1) of the problem. k_0 is the energy-intensive machine.

Appendix B. Summary performance comparisons relative to ILP-fsws in different density instances and various α values.

The following tables record summary performance comparisons of the methods *LBBD-cpws*, *LBBD-fsws*, *ILP-cpws*, and *CP* compared to the *ILP-fsws*. The gaps are calculated using equation (6.1). Each table logs the results for a given instance density. The results are expressed as percentages.

α	Metric	LBBB-fsws	LBBB-cpws	CP	ILP-cpws
0.25	mean (std)	1.12 (32.03)	14.03 (15.91)	12.58 (13.29)	5.80 (24.05)
	median [min, max]	9.81 [-84.93, 48.47]	12.63 [-56.93, 58.00]	12.11 [-36.06, 43.12]	11.20 [-77.41, 40.09]
0.5	mean (std)	-0.34 (35.80)	6.20 (32.28)	12.25 (22.94)	2.49 (34.29)
	median [min, max]	3.82 [-111.50, 62.14]	11.95 [-110.40, 62.27]	12.11 [-95.01, 62.27]	10.45 [-124.29, 61.73]
0.75	mean (std)	-8.84 (92.63)	10.98 (31.36)	0.72 (79.75)	-6.77 (80.77)
	median [min, max]	10.45 [-427.68, 82.49]	12.54 [-84.49, 81.73]	11.80 [-318.18, 92.29]	10.18 [-310.28, 92.06]
1.0	mean (std)	30.92 (25.36)	31.81 (24.63)	23.78 (19.13)	19.51 (13.93)
	median [min, max]	35.54 [0.00, 91.47]	35.54 [0.00, 91.47]	27.52 [-10.15, 69.83]	23.33 [0.00, 41.43]

Table B.6: Summary Performance Comparison Relative to ILP-fsws in sparse instances across different α values.

Set	$\alpha = 0.25$				$\alpha = 0.5$			
	LBBB-fsws	LBBB-cpws	CP	ILP-cpws	LBBB-fsws	LBBB-cpws	CP	ILP-cpws
1	0.00	0.00	0.00	0.00	0.00	0.00	0.00	0.00
2	0.00	0.00	0.00	0.00	0.00	0.00	0.00	0.00
3	1.96	2.29	2.29	2.29	1.43	1.61	1.61	1.43
4	17.06	9.90	12.73	10.31	16.88	18.94	15.77	9.25
5	0.03	9.23	9.23	9.11	0.97	9.18	12.50	8.52
6	10.43	10.72	4.99	4.07	11.06	11.26	9.16	5.13
7	0.00	20.22	22.35	16.24	0.00	12.04	20.56	14.57
<i>mean</i>	<i>4.21</i>	7.48	<i>7.37</i>	<i>6.00</i>	<i>4.33</i>	<i>7.57</i>	8.51	<i>5.56</i>
Set	$\alpha = 0.75$				$\alpha = 1.0$			
	LBBB-fsws	LBBB-cpws	CP	ILP-cpws	LBBB-fsws	LBBB-cpws	CP	ILP-cpws
1	0.00	0.00	-0.52	0.00	0.00	0.00	-0.77	0.00
2	0.00	0.00	0.00	0.00	0.00	0.00	-0.94	0.00
3	0.08	1.07	0.80	0.80	0.00	0.00	-0.80	0.00
4	20.19	19.62	19.01	20.15	19.52	19.52	15.48	19.08
5	23.82	11.37	15.89	10.33	23.39	23.39	19.42	12.88
6	11.43	4.83	8.85	5.26	11.58	11.58	7.54	5.26
7	0.00	17.03	19.42	17.79	31.86	19.04	22.59	12.85
<i>mean</i>	<i>7.93</i>	<i>7.70</i>	9.06	<i>7.76</i>	12.33	<i>10.50</i>	<i>8.93</i>	<i>7.15</i>

Table B.7: Performance Comparison Relative to ILP-fsws in dense instances across different α values. The results are given as percentages. The best approach mean value is reported in bold.

α	Set	Objective value [-]					CP	Computation Time [s]					CP	Gap to LB [%]					
		LBBB-cpws	LBBB-fswws	ILP-cpws	ILP-fswws			LBBB-cpws	LBBB-fswws	ILP-cpws	ILP-fswws			LBBB-cpws	LBBB-fswws	ILP-cpws	ILP-fswws	CP	
0.25	1	1.08459	1.08459	1.08459	1.08459	1.08459	178.35	142.49	67.02	25.77	367.88	0.00	0.00	0.00	0.00	23.88			
	2	1.05467	1.05347	1.05711	1.07605	1.05601	464.53	360.89	297.64	370.35	960.56	0.96	0.57	0.89	2.41	4.07			
	3	1.06667	1.06667	1.07921	1.10527	1.07006	1432.40	1265.24	1569.04	1399.43	1770.83	6.05	4.28	11.16	12.38	23.80			
	4	1.05495	1.05516	1.07100	1.14111	1.05721	TLR	1705.32	TLR	TLR	TLR	14.69	14.88	19.35	25.20	11.34			
	5	1.04678	1.04650	1.05646	1.12872	1.04687	TLR	1784.21	TLR	TLR	TLR	19.08	19.95	21.42	28.60	16.32			
	6	1.04828	1.05226	1.06781	1.15726	1.04766	TLR	TLR	TLR	TLR	TLR	22.61	24.32	25.92	32.04	32.52			
	7	1.06165	1.06347	1.07276	1.14009	1.06020	TLR	TLR	TLR	TLR	TLR	26.82	26.68	28.06	32.46	41.61			
	8	1.07316	1.07916	1.08463	1.15521	1.07170	TLR	TLR	TLR	TLR	TLR	27.78	28.27	29.16	33.48	36.89			
	9	1.05319	1.06026	1.06506	1.11939	1.04996	TLR	TLR	TLR	TLR	TLR	28.91	29.45	30.14	33.60	18.82			
	10	1.04521	1.04896	1.05841	1.09590	1.04142	TLR	TLR	TLR	TLR	TLR	30.06	30.29	31.24	33.55	33.10			
0.50	1	1.14210	1.14210	1.14210	1.14210	1.14210	134.38	92.33	132.01	83.30	691.13	0.00	0.00	0.00	0.00	45.16			
	2	1.10886	1.10925	1.11187	1.11494	1.11050	540.47	538.26	894.41	881.49	1525.00	0.61	0.72	2.41	2.62	12.21			
	3	1.13465	1.13475	1.14310	1.16536	1.13480	1699.58	1637.50	TLR	1699.11	TLR	8.96	8.60	11.63	12.58	52.53			
	4	1.10729	1.10919	1.11066	1.18315	1.10726	TLR	TLR	TLR	TLR	TLR	12.99	12.93	13.90	19.59	23.87			
	5	1.09057	1.09539	1.09541	1.15150	1.08978	TLR	TLR	TLR	TLR	TLR	15.59	16.00	15.56	20.30	36.75			
	6	1.08992	1.09048	1.10380	1.17400	1.08908	TLR	TLR	TLR	TLR	TLR	16.55	16.50	17.93	22.83	68.94			
	7	1.11570	1.11691	1.12770	1.17556	1.11267	TLR	TLR	TLR	TLR	TLR	19.39	19.45	20.40	23.65	79.02			
	8	1.14267	1.14828	1.15498	1.20084	1.13642	TLR	TLR	TLR	TLR	TLR	21.08	21.54	22.29	25.29	69.19			
	9	1.10116	1.10891	1.10761	1.14470	1.09682	TLR	TLR	TLR	TLR	TLR	20.42	20.94	21.11	23.69	36.01			
	10	1.08592	1.09129	1.08998	1.11778	1.08038	TLR	TLR	TLR	TLR	TLR	20.84	21.24	21.29	23.24	63.55			
0.75	1	1.13832	1.13832	1.13832	1.13832	1.13832	98.15	69.06	114.65	68.40	907.68	0.00	0.00	0.00	0.00	75.51			
	2	1.13034	1.13034	1.13096	1.13116	1.13071	700.31	568.57	991.17	1045.80	1771.83	0.66	0.54	1.90	2.06	26.07			
	3	1.15027	1.15027	1.15434	1.16677	1.15428	1710.74	1733.25	TLR	TLR	TLR	7.72	7.37	9.39	10.41	88.32			
	4	1.11488	1.11590	1.12886	1.16646	1.11835	TLR	TLR	TLR	TLR	TLR	8.29	8.30	9.82	12.56	39.73			
	5	1.11435	1.11485	1.12757	1.15514	1.11934	TLR	TLR	TLR	TLR	TLR	9.87	9.94	11.15	13.21	60.60			
	6	1.12031	1.12293	1.13507	1.18193	1.12237	TLR	TLR	TLR	TLR	TLR	10.53	11.06	12.20	15.58	107.24			
	7	1.12790	1.13121	1.14915	1.21373	1.14636	TLR	TLR	TLR	TLR	TLR	12.23	12.50	14.22	18.13	112.43			
	8	1.14792	1.15644	1.17410	1.24731	1.16143	TLR	TLR	TLR	TLR	TLR	14.36	14.96	16.21	20.70	98.58			
	9	1.12109	1.12507	1.13450	1.16628	1.12337	TLR	TLR	TLR	TLR	TLR	13.13	13.43	14.13	16.28	51.36			
	10	1.10932	1.12277	1.11372	1.14054	1.10646	TLR	TLR	TLR	TLR	TLR	13.08	14.08	13.47	15.41	91.13			
1.00	1	18836.80	18836.80	18836.80	18836.80	18836.80	51.53	4.84	51.15	7.74	998.41	0.00	0.00	0.00	0.00	109.78			
	2	35193.71	35193.71	35193.71	35193.71	35228.92	62.25	5.71	63.92	14.88	TLR	0.00	0.00	0.00	0.00	38.52			
	3	50475.65	50475.65	50475.65	50475.65	50475.65	50638.29	64.07	19.00	74.00	59.52	TLR	0.00	0.00	0.00	0.00	127.94		
	4	63513.12	63513.12	63513.12	63513.12	63513.12	63796.35	67.12	22.27	84.97	142.12	TLR	0.00	0.00	0.00	0.00	55.36		
	5	76038.46	76038.61	76038.46	76038.46	76038.46	76934.01	79.66	48.57	136.01	291.34	TLR	0.00	0.00	0.00	0.00	80.66		
	6	108774.14	108773.36	108774.14	108773.36	108774.14	10951.58	93.83	68.09	233.27	575.61	TLR	0.00	0.00	0.00	0.00	141.36		
	7	109975.28	109975.28	109974.88	111356.78	112242.49	131.14	154.96	377.13	1168.95	TLR	0.00	0.00	0.01	1.29	159.26			
	8	122464.93	122464.93	122464.93	122464.93	122464.93	130829.26	126524.27	136.75	140.97	588.31	1463.10	TLR	0.00	0.00	0.01	5.64	135.43	
	9	172043.69	172043.69	172043.69	180534.61	178107.52	319.43	433.17	890.01	1364.18	TLR	0.01	0.02	0.05	4.92	62.31			
	10	181718.22	181718.22	181718.61	200837.76	187039.61	354.55	425.82	949.23	1741.61	TLR	0.00	0.00	0.02	8.45	120.06			
	11	177171.48	177171.48	177965.55	196135.81	182976.83	343.48	544.91	1160.51	TLR	TLR	0.00	0.01	0.51	9.73	90.87			
	12	211589.57	211589.57	218542.68	242079.98	219796.09	414.36	568.70	1636.85	TLR	TLR	0.00	0.00	3.46	13.94	104.28			
	13	192963.33	192963.33	195283.94	225686.43	199865.81	667.37	867.26	1663.35	TLR	TLR	0.00	0.01	1.62	15.17	100.21			
	14	236045.06	236045.89	238656.60	281722.66	248602.32	802.14	1091.94	1728.91	TLR	TLR	0.04	0.05	0.85	17.90	158.59			
	15	242280.91	244605.33	248601.78	290132.66	256490.90	1079.60	1220.56	1722.13	TLR	TLR	0.04	1.41	2.33	21.77	238.89			

Table B.8: Detailed results of the experiments of the standard instance sets. The results are aggregated across instances of a set, and the average objective, computation time (in seconds), and best gap to lower bound (in percentage) values are reported. There are 20 instances per set. The characteristics of the sets are described in Table 2. “TLR” = Time Limit Reached.